Monitoring cork and holm oak woodlands with Google Earth Engine

Valentine Aubard

AGROCAMPUS OUEST

☐ **CFR Angers**

☑ **CFR Rennes**

Année universitaire : 2017-2018

Spécialité : Ingénieur agronome et territorial (Vetagro-Sup)

Spécialisation (et option éventuelle) :

Télédétection et environnement (TELENVI, Agrocampus-Ouest)

Mémoire de Fin d'Études

☐ d'Ingénieur de l'Institut Supérieur des Sciences agronomiques, agroalimentaires, horticoles et du paysage

☐ de Master de l'Institut Supérieur des Sciences agronomiques, agroalimentaires, horticoles et du paysage

☑ d'un autre établissement (étudiant arrivé en M2)

Monitoring cork and holm oak woodlands with Google Earth Engine

Par : Valentine AUBARD

Soutenu à Rennes le 13 septembre 2018

Devant le jury composé de :

Présidents : Hervé Nicolas, Samuel Corgne

Maîtres de stage : João Manual Das Neves Silva, Joana Amaral Paulo

Enseignant référent : Hervé Nicolas

Autres membres du jury (Nom, Qualité) :

Rodéric Béra, Maitre de Conférence

Hervé Squividant, Ingénieur

Les analyses et les conclusions de ce travail d'étudiant n'engagent que la responsabilité de son auteur et non celle d'AGROCAMPUS OUEST

Fiche de confidentialité et de diffusion du mémoire

Confidentialité

☒ Non ☐ Oui si oui : ☐ 1 an ☐ 5 ans ☐ 10 ans

Pendant toute la durée de confidentialité, aucune diffusion du mémoire n'est possible (1).

Date et signature des maîtres de stage (2) :

INSTITUTO SUPERIOR D AGRONOMIA 03/09/2018
Universidade de Lisboa
Gabinete de Relações Internacionais
International Relations Office

A la fin de la période de confidentialité, sa diffusion est soumise aux règles ci-dessous (droits d'auteur et autorisation de diffusion par l'enseignant à renseigner).

Droits d'auteur

L'auteur(3) **Valentine AUBARD**
autorise la diffusion de son travail (immédiatement ou à la fin de la période de confidentialité)

☒ Oui ☐ Non

Si oui, il autorise

☐ la diffusion papier du mémoire uniquement(4)

☐ la diffusion papier du mémoire et la diffusion électronique du résumé

☒ la diffusion papier et électronique du mémoire (joindre dans ce cas la fiche de conformité du mémoire numérique et le contrat de diffusion)

(Facultatif) ☒ accepte de placer son mémoire sous licence Creative commons CC-By-Nc-Nd (voir Guide du mémoire Chap 1.4 page 6)

Date et signature de l'auteur : 03/09/2018

Autorisation de diffusion par le responsable de spécialisation ou son représentant

L'enseignant juge le mémoire de qualité suffisante pour être diffusé (immédiatement ou à la fin de la période de confidentialité)

☒ Oui ☐ Non

Si non, seul le titre du mémoire apparaîtra dans les bases de données.

Si oui, il autorise

☐ la diffusion papier du mémoire uniquement(4)

☐ la diffusion papier du mémoire et la diffusion électronique du résumé

☒ la diffusion papier et électronique du mémoire

Date et signature de l'enseignant : (H. NICOLAS)

(1) L'administration, les enseignants et les différents services de documentation d'AGROCAMPUS OUEST s'engagent à respecter cette confidentialité.
(2) Signature et cachet de l'organisme
(3) Auteur = étudiant qui réalise son mémoire de fin d'études
(4) La référence bibliographique (= Nom de l'auteur, titre du mémoire, année de soutenance, diplôme, spécialité et spécialisation/Option)) sera signalée dans les bases de données documentaires sans le résumé

Abstract

Oak woodlands are being documented to be declining in southern Europe. In order to verify and quantify this phenomenon, 34-year trends of the Normalized Difference Vegetation Index (NDVI) were calculated and mapped at 30-meter pixel scale for all cork oak (*Quercus suber*) and holm oak (*Quercus ilex*) areas of continental Portugal.

NDVI is considered a good proxy to monitor trees health and productivity along years. Landsat 5, 7 and 8 imagery from 1984 to 2017 were used to derive a long-term NDVI time series. MODIS 250-m spatial resolution NDVI product was used to compare values for the period after 2000. All imagery were freely available and treatable on Google Earth Engine. NDVI values of Landsat 5 and 8 were adjusted to Landsat 7 values. Only July and August NDVI were used to minimize the spectral contribution of understorey vegetation and its phenological variability, thus focusing on the tree layer. Signs and significance of trends were calculated by Mann-Kendall (MK) and contextual MK tests, and their slopes using Theil-Sen (TS) estimator. The methodological approach was first tested on six cork oaks stands. Linear models revealed the effect of annual cumulated precipitation and debarking on NDVI variations. All trends were found significant. A Pettitt test showed significant change-points around the year 2000. At country scale, a spatio-temporal trend analysis was performed on stable cover areas of holm and cork oak. Thirty percent of woodlands area presents declining trends, mainly located in Centro region, and interior and littoral of Alentejo.

Keywords: *Quercus suber* L., *Quercus ilex* L., Montado, Time series, Normalized Difference Vegetation Index, Contextual Mann-Kendall, Portugal

Résumé

Introduction/Etat de l'art – De nombreux articles scientifiques décrivent le déclin des forêts de chênes du Sud de l'Europe. Les chênes lièges (*Quercus suber L.*) et chênes verts (*Quercus ilex L.*) couvrent un tiers du Portugal continental, et ont une grande valeur économique, sociale et environnementale pour le territoire. Les chênes lièges sont surtout exploités pour le liège, matériel utilisé pour les bouchons de bouteilles et l'isolation, dû à son élasticité et sa faible perméabilité. Il est extrait de l'arbre adulte tous les 9 ans ou plus. Le Portugal possède 50% du marché mondial. Les chênes verts produisent de riches glands utilisés pour l'alimentation animale, en plus de protéger le bétail du froid en hiver et du soleil en été. Le potentiel de la télédétection et de la plateforme Google Earth Engine (GEE) ont été utilisés pour établir les tendances de productivité de ces deux espèces sur une longue période et pour tout ~~un~~/le pays. GEE permet de manipuler gratuitement en ligne des données rasters et vecteurs du monde entier. Cette étude permet d'évaluer ses performances pour le traitement d'image appliqué au suivi des parcelles forestières. L'indice de végétation par différence normalisé NDVI (Normalized Difference Vegetation Index) a déjà prouvé être un bon proxy pour suivre la production et la santé des forêts méditerranéennes de chênes. Il sera utilisé à une échelle spatiale adaptée, bien plus précise que les précédentes études.

Objectifs et Plan – L'objectif principal de ce travail était de quantifier spatialement le déclin annoncé des chênes et de délivrer une carte des tendances sur 34 ans de toutes les parcelles de chênes lièges et de chênes verts du Portugal continental. Le second objectif était de comprendre les principales variables expliquant les variations de NDVI au fil des ans. Pour ce faire, la première partie du travail a été d'établir une méthodologie pour extraire des tendances de séries temporelles, de l'appliquer et de la valider à l'échelle de la parcelle, en suivant les NDVI de six peuplements de chênes lièges portugais, et de trouver des variables explicatives pour ces variations. La seconde partie fut d'appliquer cette méthode pour cartographier les tendances de NDVI de ces deux espèces pour toute l'aire du Portugal continental.

Partie 1 – Matériel et méthodes. Six parcelles de chêne liège de 1 hectare furent sélectionnées pour leur diversité de production de liège, leur densité, leur localisation, leur sol et végétation de sous-étage. Les images SR Tier 1 des capteurs Landsat -5, -7 et -8 furent utilisées pour calculer les NDVI à une résolution spatiale de 30 mètres, entre 1984 et 2017, tous les 16 jours. Une fonction *Fmask* leurs a été appliquée pour ôter nuages et ombres. La version 6 du produit MODIS Terra Vegetation Indices, qui fournit les NDVI à 250 mètres de résolution fut utilisée pour comparer les résultats. Un ajustement des valeurs de NDVI entre les différents capteurs Landsat était nécessaire dû aux différences de sensibilité de longueur d'onde des bandes utilisées. Des équations spécifiques à chaque parcelle furent établies et leur fiabilité comparée aux équations proposées de la littérature. Seule une moyenne des valeurs de NDVI des mois de Juillet et Août a été utilisée pour l'analyse, période pendant laquelle les valeurs de NDVI de la végétation de sous-étage sont minimales, tandis que celles des arbres ne varient que peu pendant l'année. Les tendances d'évolution des valeurs de NDVI au cours du temps (en année) étant supposées monotones, le test non-paramétrique de Mann-Kendall et l'estimateur de Theil-Sen furent utilisés pour estimer la significativité, le signe des tendances et leur vitesse d'évolution (pente). Un test de Pettitt a été appliqué pour détecter d'éventuelles ruptures de tendance. Des modèles linéaires multiples furent établis pour tester l'effet sur les valeurs de NDVI de la quantité de précipitations, cumulées par an ou par saison, et de l'extraction du liège.

Partie 1 – Résultats et discussion. Pour ajuster les valeurs de NDVI entre les différents capteurs Landsat, l'équation proposée par Ju *et al.* (2016) entre Landsat-5 et -7 se révéla la meilleure et utilisable à large échelle. Entre Landsat-7 et -8, seules les équations établies pour chaque site d'étude semblèrent corriger efficacement la différence, et furent retenues pour les analyses de la Partie 1, mais les valeurs de NDVI de Landsat-8 ne furent pas utilisées pour l'ensemble du Portugal. La comparaison

des NDVI des capteurs Landsat et MODIS sur la période 2000-2017 a permis de valider ces choix. La quantité annuelle de précipitations (entre Août de l'année précédente et Juillet) révéla être corrélée positivement et significativement à la moyenne de NDVI de Juillet-Août, les quantités de précipitations au printemps et en été étant les plus déterminantes. Cela concorde avec les relations déjà mises en évidence entre précipitations et productivité des arbres (en quantité de liège). L'extraction du liège (entre Juin et Août) l'année précédente semble avoir un impact significatif négatif sur la moyenne de NDVI de Juillet-Aout. L'extraction la même année n'eut pas d'effet significatif. Cela laisse supposer que le chêne va d'abord investir son énergie dans la production de nouveau liège, nécessaire à sa régulation hydrique et sa protection contre les feux, au printemps suivant, plutôt que dans la production de nouvelles feuilles, qui peut être différée en automne. Les tendances obtenues pour les six sites d'étude ont été significatives et leurs signes et taux cohérents avec la production de liège connue pour chaque parcelle. Deux sites présentent des tendances négatives, qui peuvent indiquer une diminution de la densité de la parcelle ou un stress des arbres de plus en plus important au fil du temps, avec répercussion sur le feuillage. Des ruptures de tendances significatives ont été trouvées pour chaque parcelle, oscillant entre 1996 et 2005, ce qui suggère une rupture de tendance dans les variables influençant les valeurs de NDVI des chênes lièges et chênes verts autour de l'an 2000.

Partie 2 – Matériel et méthodes. Seuls furent utilisés les peuplements de chênes lièges et chênes verts gardant la même classe d'occupation du sol au cours du temps, déterminés grâce aux cartes d'utilisation et d'occupation des sols portugaises (Carta de Uso e Ocupação do Solo (COS)) de 1995, 2007, 2010 et 2015. La classification très précise des COS fut simplifiée en cinq classes : forêts de chênes lièges, forêts de chênes verts, systèmes agroforestiers (SAF) de chênes lièges, SAF de chênes verts et SAF où coexistent les deux espèces. Un masque des aires ayant subi un ou plusieurs feux de forêts entre 1984 et 2017 fut ensuite appliqué. Suivant les résultats de la Partie 1, seuls les moyennes de NDVI de Juillet-Août des capteurs Landsat-5 (valeurs ajustées selon l'équation proposée par Ju *et al.* (2016)) et Landsat-7 furent utilisées pour établir les séries temporelles par pixel de 1984 à 2017. Le test de Mann-Kendall a été utilisé pour obtenir le signe et la significativité des tendances, ainsi que le test contextuel de Mann-Kendall, prenant en compte les pixels voisins pour estimer la significativité. L'estimateur de Theil-Sen fut ensuite appliqué pour obtenir la vitesse d'évolution (pente).

Partie 2 – Résultats et discussion. La carte des tendances significatives et non-significatives des peuplements de chênes lièges et chênes verts fut obtenue pour le territoire continental portugais, excepté les aires inférieures à l'aire unitaire minimale des COS (1ha). De même, les feux de forêts d'aire inférieure à 5ha ne furent pas masqués. Aucune COS n'existe avant 1995 pour assurer que les classes d'occupation des parcelles retenues n'évoluèrent pas entre 1984 et 1995. Le type de production et la législation portugaise actuelle assurent néanmoins une grande stabilité de ce couvert dans le temps. Cette carte indique des zones en déclin notamment dans la région Centro, le littoral et l'intérieur de l'Alentejo. Sur toute l'aire traitée, trente pour cent des tendances significatives sont décroissantes, indiquant la mort de certains arbres (diminuant la densité de la canopée) ou une diminution de plus en plus drastique de la capacité photosynthétique des arbres chaque été. Par classe, les SAF de chênes lièges donnèrent le pourcentage de tendances significatives négatives le plus élevé ; les SAF de chênes verts donnèrent le plus bas. Cette différence peut s'expliquer par la plus grande capacité d'adaptation des chênes verts à des conditions xérophytiques, notamment dans les SAF, de faible densité. Un abandon progressif des SAF de chênes lièges pourrait également expliquer ce résultat. Un élargissement de la carte a été fait autour de chaque site étudié en Partie 1 pour visualiser les différences entre les résultats des tests de Mann-Kendall et contextuel de Mann-Kendall, globalement similaires. Les résultats des Parties 1 et 2 furent cohérents, et les élargissements mirent en évidence l'importante corrélation spatiale mais également la grande variabilité des tendances de pixels proches. Cette variabilité pourrait être expliquée seulement par une étude exhaustive des sites, prenant en compte divers facteurs comme la pente, l'exposition, la texture et la lithologie des sols, l'âge des arbres, les potentielles maladies et la gestion humaine (de la végétation de sous-étage, du pâturage et

de l'extraction du liège). Bien évidemment, une étude aussi précise peut difficilement être réalisée à l'échelle d'un pays.

Conclusion – Ce travail a montré les avantages et les faiblesses de Google Earth Engine pour le suivi forestier. La méthodologie adoptée pour ce travail a permis d'établir une carte détaillée des tendances sur 34 ans de l'indice NDVI, vu comme un proxy de la productivité, pour deux espèces d'arbres, à l'échelle d'un pays entier. Pour un suivi à haute échelle de résolution spatiale sur un site de taille raisonnable, cette méthodologie peut être améliorée en prenant en compte le pourcentage de couvert de la canopée, et la composition de la végétation de sous-étage au cours du temps, et ainsi évaluer la part du couvert arboré dans les valeurs de NDVI. Cette méthode peut être reproduite et adaptée à d'autres indices de végétation, d'autres espèces, d'autres lieux et d'autres problématiques. Les résultats donnent un signal d'alerte et pointent les besoins d'une meilleure compréhension du déclin observé, ainsi que de la recherche de solutions dans un contexte de réchauffement climatique.

Acknowledgements

Special thanks to my supervisors, Joana Amaral Paulo, João Manuel Das Neves Silva and to their respective teams, for their guidance, ideas, advises, and continual support. This research was carried out in the *Centro de Estudos Florestais* (Forest Research Centre) of the *Instituto Superior de Agronomia* (School of Agriculture), University of Lisbon.

Thanks to my referent teacher Hervé Nicolas, professor of Agrocampus-Ouest school, for his support and advises. Acknowledgements are also due to my various teachers of Vetagro-Sup, Agrocampus-Ouest and the University of Rennes 2 for sharing their knowledge and for their patience.

At last, thanks to the Auvergne-Rhône-Alpes region and to the Erasmus+ program for their financial support which made this six-month internship possible.

List of Figures

Figure 1: Localization of the six cork oak stands in Portugal. 3
Figure 2: Cumulated precipitation from August to next July (mm) per study-site, from the closest climate stations. 5
Figure 3: Methodology to adjust the NDVI values derived from different Landsat sensors. 7
Figure 4: Comparison of adjusted-Landsat and MODIS NDVI variation along years. 13
Figure 5: Mean cork production in millimetres per year per plot function of 34-year NDVI trends (from 1984 to 2017). 17
Figure 6: Landsat NDVI summer means per year for each study-site. 18
Figure 7: Masks of constant land cover classes (left) and burned areas (right) 21
Figure 8: Mann-Kendall test results - signs and significance 23
Figure 9: Frequency histogram of significant and not significant slope (left), and significant slopes only (right), for the 5 classes of land use. 24
Figure 10: Theil-Sen slopes and Mann-Kendall significance. 25
Figure 11: Theil Sen slopes and Mann-Kendall significance maps per land cover class. 26
Figure 12: Theil-Sen slopes around the six study-sites, with Mann-Kendall and Contextual Mann-Kendall significance 28

List of Tables

Table 1: Characteristics of the six stands. 4
Table 2: Most recent debarking dates for the six study-sites. 5
Table 3: Image collections used in Google Earth Engine. 6
Table 4: Bibliographic equations of adjustment. 8
Table 5: Determined site-specific NDVI adjustment equations between Landsat sensors. 8
Table 6: Percentages of absolute differences in means (%D means) and medians (%D medians) between Landsat-5 and Landsat-7 NDVI. 12
Table 7: Percentages of absolute differences in means (%D means) and medians (%D medians) between Landsat-8 and Landsat-7 NDVI. 12
Table 8: Parameter estimates for the $NDVI_t$ model (Equation 2). 15
Table 9: Parameter estimates for the $NDVI_t$ model (Equation 3). 15
Table 10: Parameter estimates for the $NDVI_t$ model (Equation 4). 15
Table 11 : Pearson's correlation and Mann-Kendall Tau. 16
Table 12: Linear trend (L) and Theil Sen estimator (TS) comparison. 17
Table 13: Results of Pettitt change-point test per study-site for Landsat time-series (1984- 2017). 19
Table 14: Five classes used to summarise the classification of the COS. 21
Table 15: Area and percentage of total area of Mann-Kendall map results. 22
Table 16: Means of Theil-Sen slope per class 24
Table 17: Percentage of significant and positive trends per land cover class 27

List of Appendix

Appendix 1: *Fmask* function coded in Google Earth Engine following pixel quality values. I
Appendix 2: Comparison of bands of Landsat and MODIS sensors. II
Appendix 3: Comparison of NDVI values for cork oaks, herbaceous and shrubs along years. III
Appendix 4: Normal Q-Q plots for the six study-site, for Landsat-5, -7 and -8 derived-NDVI raw-values. IV
Appendix 5: Boxplots to compare the accuracy of NDVI adjustment equations between Landsat-5, -7 and -8 sensors. V
Appendix 6: Comparison of adjusted and not-adjusted Landsat -5 and -8 NDVIs. VI
Appendix 7: Matches between the classes kept (Code) and the original classes of the Portuguese land use and land cover maps (*Carta de Uso e Ocupação do Solo* (COS)) for 1995, 2007-2010 and 2015 classifications. VII
Appendix 8: Evolution of area covered per each class of land cover, and comparison with the amount of constant areas of each class. VIII
Appendix 9: Enlargement of the masks of constant land cover classes and burned areas. IX
Appendix 10: Enlargement of Theil Sen slopes and Mann-Kendall significance maps per land cover class. XI
Appendix 11: Frequency histograms of all slopes and significant slopes values for each land cover class. XVI

Table of contents

Introduction 1

Part 1: NDVI trends at plot scale 3

1. Material and methods 3

1.1 Study-site characterization 3

1.2 Satellite image characterization 3

1.3 NDVI and adjustment between Landsat sensors 6

1.4 Months used to establish trends 9

1.5 Effect of precipitation and debarking on trees NDVI 9

2. Results and Discussion 11

2.1 Best NDVI-adjustment equations 11

2.2 Evolution of NDVI values along years 11

2.3 Explaining NDVI variations with precipitation and debarking 11

2.4 Significant NDVI trends for the six study-sites 14

2.5 Rate of change of the trends 16

2.6 Trend change-point 19

3. Conclusion of Part 1 19

Part 2: Mapping NDVI trends for continental Portugal 20

4. Material and methods 20

4.1 Selected areas 20

4.2 Images, NDVI and time series 20

5. Results and Discussion 22

5.1 Mann-Kendall for all cork oak and holm oak woodlands in Portugal 22

5.2 Theil Sen slope for all Portugal 22

5.3 Mann-Kendall and Theil-Sen results per class of land cover 24

5.4 Application to the study-sites and Contextual Mann-Kendall 27

6. Conclusion of Part 2 27

General Conclusion 29

References 30

Introduction

An important decline of oaks species have been noticed in the last decades in Portugal due to various possible factors such as land management, especially livestock grazing (Godinho *et al.,* 2016), difficult access to ground water in summer in hilltops and shallow soils (Costa *et al.,* 2010), climate change (Kim *et al.,* 2017), associated to pests and diseases (Brasier *et al.*, 1993; Romero *et al*., 2007). This decline has been observed in several ecosystem variables such has the number of trees per hectare (Costa *et al*., 2009; Silva J. S., 2007), tree regeneration, tree canopy cover (Paulo *et al.,* 2015a) or cork growth (Paulo *et al.,* 2017).

Woodlands of cork oak (*Quercus suber L*.) and holm oak (*Quercus ilex L.*) cover one third of woodland areas of the continental territory of Portugal, mostly as an artificial extensive silvopastoral system called *montado* (ICNF, 2013). They have an important value for Portugal's economy, society and environment, providing various ecosystem services as landscape and tourism hotspots, reducing fire risk and soil erosion, increasing carbon sequestration and key-habitats for rare and endemic species (Moreno *et al.,* 2017; Da Silva *et al.*, 2009).

Cork oaks are exploited mainly for cork, but under the typical silvopastoral management system acorns are also a valuable product for animal feeding. Cork is one of the most valuable product of non-wood forest exploitation worldwide, having remarkable mechanics properties as low permeability to liquids and gases, rot-proof and important elasticity (Pereira, 2007). It is used mainly for bottle stoppers, although isolation uses can also be applied. Also, an emerging clothing market and other products have been expanding. Portugal is the main producer in the world, with 50% of the global market, and the sector contribute to 3% of the gross domestic product of the country, providing a considerable amount of job positions specially on rural areas. Workable cork, the third stripping since the first two don't have a proper properties, is extracted from adult trees – from 50 to 150 years old, sometimes the double – with a minimal gap of 9 years between each debarking according to the current national legislation in Portugal.

Holm oaks produce characteristic acorns that are used to feed livestock, in particular black pigs which are associated with these stands and produce premium meat, or for culinary purposes. The trees are also good shelter either in winter, against frost, either in summer against heat and sun exposure. Holm oak wood is known to be extremely calorific and is traditionally used as firewood. Also, before the development of fossil fuel, holm wood was for this reason valued for charcoal production (Rigueiro-Rodríguez *et al*., 2008; Moreno *et al*., 2017).

In order to evaluate the long-term productivity trends of those two species for a whole country, the potentialities of remote sensing and of the new open access platform Google Earth Engine (GEE) were considered to be exploited. GEE gives free access to thousands of geographic information system features (vector and raster) from all over the world. The JavaScript code editor allows to manipulate them online, without downloading, and to save images or table results on a stockage platform. Therefore, this study will be an opportunity to evaluate to what extent Google Earth Engine is adapted to the needs and purpose of image processing with the goal of forest monitoring.

A strong correlation exists between wood, leaves and seed production of North American oak species and the Normalized Difference Vegetation Index (NDVI) at 1-km of spatial resolution, from the National Oceanic and Atmospheric Administration Advanced Very High Resolution Radiometer (NOAA/AVHRR) satellite (Wang *et al.*, 2004). The Moderate Resolution Imaging Spectroradiometer

(MODIS) NDVI at 250-m of resolution was also proved to be an efficient indicators of forest biomass growth and dieback in Mediterranean holm oak forests (Ogaya *et al.,* 2015). In this study, NDVI is used as a proxy of cork and acorn productivity and of the global health of holm oak and cork oak stands.

The first objective of this work was to spatially quantify oaks decline and to deliver a map of 34-year NDVI trends for all cork oak and holm oak areas of continental Portugal. The spatial scale of this analysis had to meet the needs of plot monitoring. The second objective was to understand the main factors explaining oaks NDVI variations along years.

The work was divided in two parts: 1) establishing a methodology to extract times series trends at plot scale, following the NDVI evolution of six Portuguese cork oak woodlands, and finding explanatory variables for NDVI variations; 2) applying this method to map spatio-temporal NDVI trends of cork and holm oak areas for the whole territory of continental Portugal.

Part 1: NDVI trends at plot scale

1. Material and methods

1.1 Study-site characterization

Six pure cork oak stands were chosen throughout Portugal (**Figure 1**), contrasting in their distance to the sea, density, understorey and cork production (**Table 1**). Their cork productivity is being followed since the 90s by the group Forest Ecosystem Management Under Global Change (ForChange) of the Forest Research Centre (CEF) of the Instituto Superior de Agronomia (ISA) in Lisbon. The dates of debarking of each stand are described in **Table 2**, and cumulated precipitation per year, from 1983 to 2017, in **Figure 2**. Portugal has a Mediterranean climate with a very defined dry season in summer and mild temperature in winter.

The area of each plot is around 1 ha, thus can be fitted 11 Landsat pixels or 0.16 MODIS pixels. The areas were defined by a circular buffer of 57 m² around the center of the plot (a polygon with 24 vertices) of exactly 1.0085 ha. The center was selected in order to get the most homogeneous canopy cover possible.

Figure 1: Localization of the six cork oak stands in Portugal.

1.2 Satellite image characterization

Images from four sensors were used for this study following two objectives: 1) making the longest period available time series at the most precise spatial scale possible; 2) validating the results with images taken from a unique sensor to avoid sensor bias.

First, 30-m pixel with a 16-day cycle Landsat images from three sensors were chosen (**Table 3**) to create a time series of 34 years, between 1984 and 2017. GEE provide Top of Atmosphere (TOA) and Surface Reflectance (SR) images from Landsat-4, -5, -7 and -8. Only the already atmospherically compensated SR images were used. Landsat-4 images were ignored since the collection contains only 64 images for all Portugal between 1988 and 1993, period already covered by Landsat-5 images. For Landsat-5, -7 and -8, only the first category of data 'Tier 1' (T1) produced by the United States Geological Survey (USGS) was used, since it meets geometric and radiometric quality requirements.

Table 1: Characteristics of the six stands.

Site	Bêbeda	Contenda	Coruche	Grândola	Lezírias	Portel
Longitude (EPSG:4326)	-8.781102	-7.103938	-8.335581	-8.438551	-8.855579	-7.634190
Latitude (EPSG:4326)	38.000741	38.075716	39.139173	38.102245	38.815475	38.253932
Tree age (in 2010)	Even-aged, around 70 years old	Uneven-aged (natural regeneration), more than 100 years old	Even-aged, around 60 years old	Uneven-aged (natural regeneration), more than 100 years old	Even-aged, around 70 years old	Even-aged, 90-100 years old
Estimated canopy cover (percentage in 2010) *	13.1	8.8	18.8	7.3	23.8	12.8
Mean cork thickness ($mm.tree^{-1}.year^{-1}$) **	3.43	2.53	4.15	3.06	3.30	2.64
Understorey	Medium shrubs and herbs	Medium shrubs and herbs	Pasture, cow grazing	Pasture, sheep grazing	Abundant herbaceous	A few shrubs and herbs, sheep and cow grazing
FAO soil group ***	Arenosoils	Leptosoils	Podzols	Arenosoils and Podzols	Arenosoils	Leptosoils

* mean for each plot, according to the 30-m pixel Landsat Tree Cover Continuous Fields layer for 2010, which gives a percentage of the vertically projected area of vegetation (including leaves, stems, branches, etc.) of woody plants greater than 5 meters in height (GEE Image Collection ID: GLCF/GLS_TCC).
** from measure of rings thickness after boiling, following the methodology used by Paulo and Tomé (2010), the mean was calculated for each stand from samples of 23 to 36 trees, for two debarking periods (a total of 17 to 22 years).
*** soil group classification of IUSS working group WRB (2006).

Table 2: Most recent debarking dates for the six study-sites.

Site	Bêbeda	Contenda	Coruche	Grândola	Lezírias	Portel
Dates of debarking	1987	1988	1988	1984	1987	1984
	1997-08-13	1998-07-17	1997-06-27	1996-07-27	1996-07-11	1997-07-02
	2008-07-23	2007-06-27	2006-06-02	2006-05-25	2005-06-02	2007-06-09
	2017-08-01	/	2016-06-17	2016-06-27	2015-06-23	2016-07-07

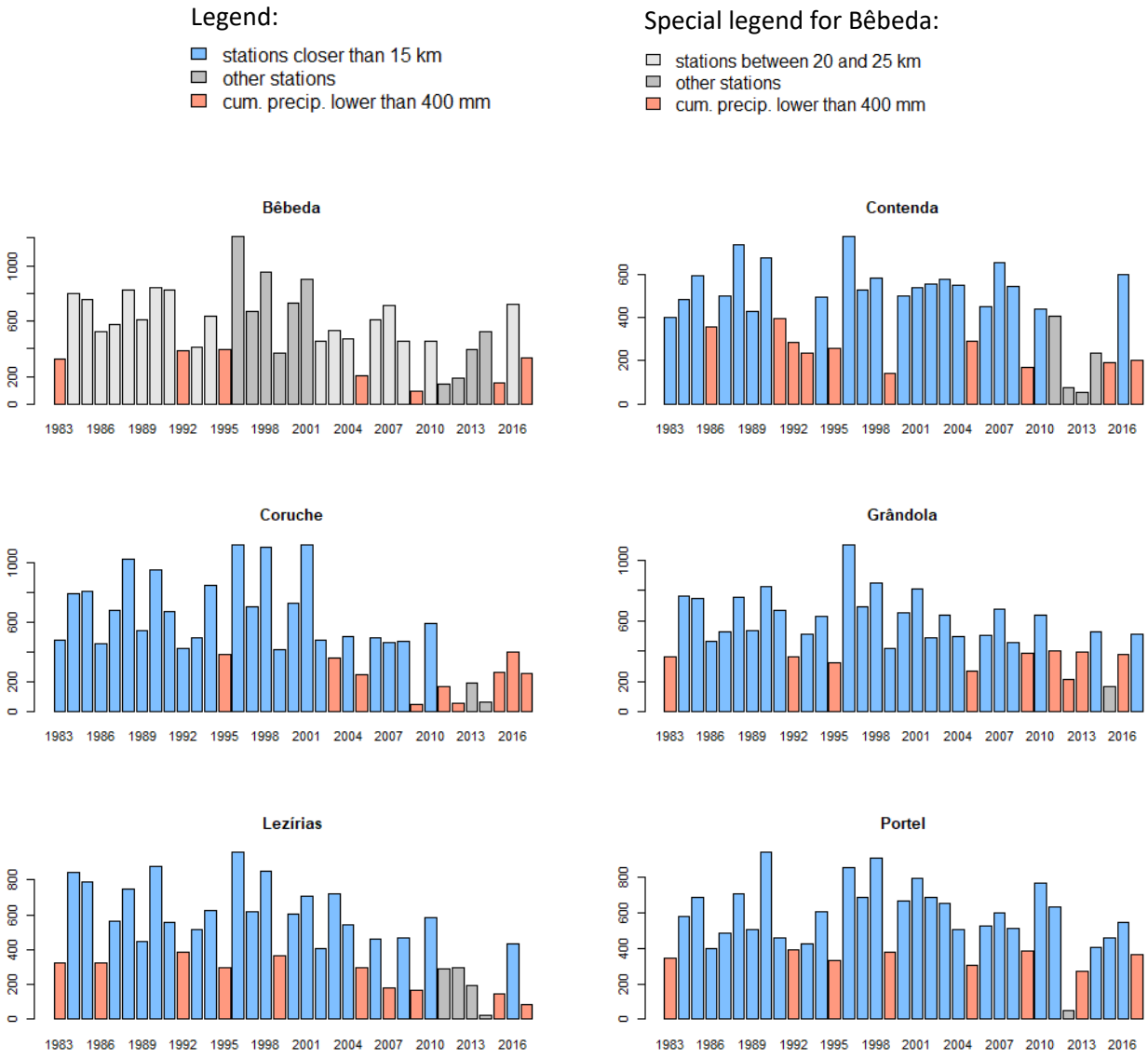

Figure 2: Cumulated precipitation from August to next July (mm) per study-site, from the closest climate stations.

The *Fmask* function (Zhu and Woodcock, 2012) was implemented in GEE to remove clouds and shadows from Landsat images, using the quality of pixel band (*pixel_qa*). The attributes of the *pixel_qa* band and the function used in GEE are presented in the **Appendix 1**. All images of Landsat-7 taken after May 31, 2003 contain "SLC-off gaps" due to the failure of the Scan Line Corrector (SLC) of the sensor. On GEE, the values of the missing pixels are informed as 'NA' values. No interpolation to fill those gaps was made. Second, version 6 of the MODIS Terra Vegetation Indices (**Table 3**) provides bands of NDVI and EVI at 250-m scale every 16 days, already fully corrected, including cloud-masked. This dataset was chosen to validate Landsat results between 2000 and 2017.

Table 3: Image collections used in Google Earth Engine.

Sensor	Range of available dates*	Time scale	Spatial scale	GEE Image Collection ID used
Landsat-5 TM	1984-01-01 - 2012-05-05	16-day cycle	30x30 m	LANDSAT/LT05/C01/T1_SR
Landsat-7 ETM+	1999-01-01 - 2018-05-31	16-day cycle	30x30 m	LANDSAT/LE07/C01/T1_SR
Landsat-8 OLI	2013-04-11 - 2018-06-14	16-day cycle	30x30 m	LANDSAT/LC08/C01/T1_SR
MODIS Terra V6 Vegetation Indices	2000-02-18 - 2018-05-25	16-day cycle	250x250 m	MODIS/006/MOD13Q1

*on 2018-06-28: new images take as much as one month to be evaluated.

1.3 NDVI and adjustment between Landsat sensors

The Normalized Difference Vegetation Index (NDVI, **Equation 1**) (Rouse *et al.*, 1974) exploits the highly reflectance of the vegetation in the near infrared (NIR) region and its strong chlorophyll absorption in the visible region.

$$NDVI = (NIR - Red) / (NIR + Red) \qquad \textbf{Equation 1}$$

where *NIR* is Landsat SR individual Near Infrared channel, respectively band 4 for Landsat-5 and -7, band 5 for Landsat-8 and *Red* is Landsat SR individual Red channel, respectively band 3 for Landsat-5 and -7, band 4 for Landsat-8.

A difference is expected between the values of the vegetation index regarding the differences of bands wavelength sensibility presented in **Appendix 2** between Landsat-5, -7 and -8. To establish trends, an adjustment between the three Landsat sensors-derived NDVI is thus essential. Some linear relations have already been established for the United States (She *et al.*, 2015, Roy *et al.*, 2016), Canada (Ju *et al.*, 2016) and Northern Europe (Steven *et al.*, 2003) (**Table 4**). The first step of this study was to select the best relations for Portugal. The accuracy of the equations selected from literature was compared with site-specific equations made for each plot (**Table 5**). Site-specific equations have been calculated for each plot adjusting Landsat-5 and Landsat-8 NDVI values to Landsat-7 values. The methodology adopted, schematically explained on the **Figure 3** below, was inspired by the tandem images cross-calibration of Ju *et al*., 2016. For each site, NDVI values were extracted from 1984-01-01 to 2017-12-31 for each pixel intersecting the buffer area. Site-specific relations were assumed linear, with an intercept equal to zero, the literature equation intercepts being very small when not null (**Table 4**). Only images values from different sensors separated by a time-gap of 8 days (minimum gap possible in Portugal) were used, backward and forward.

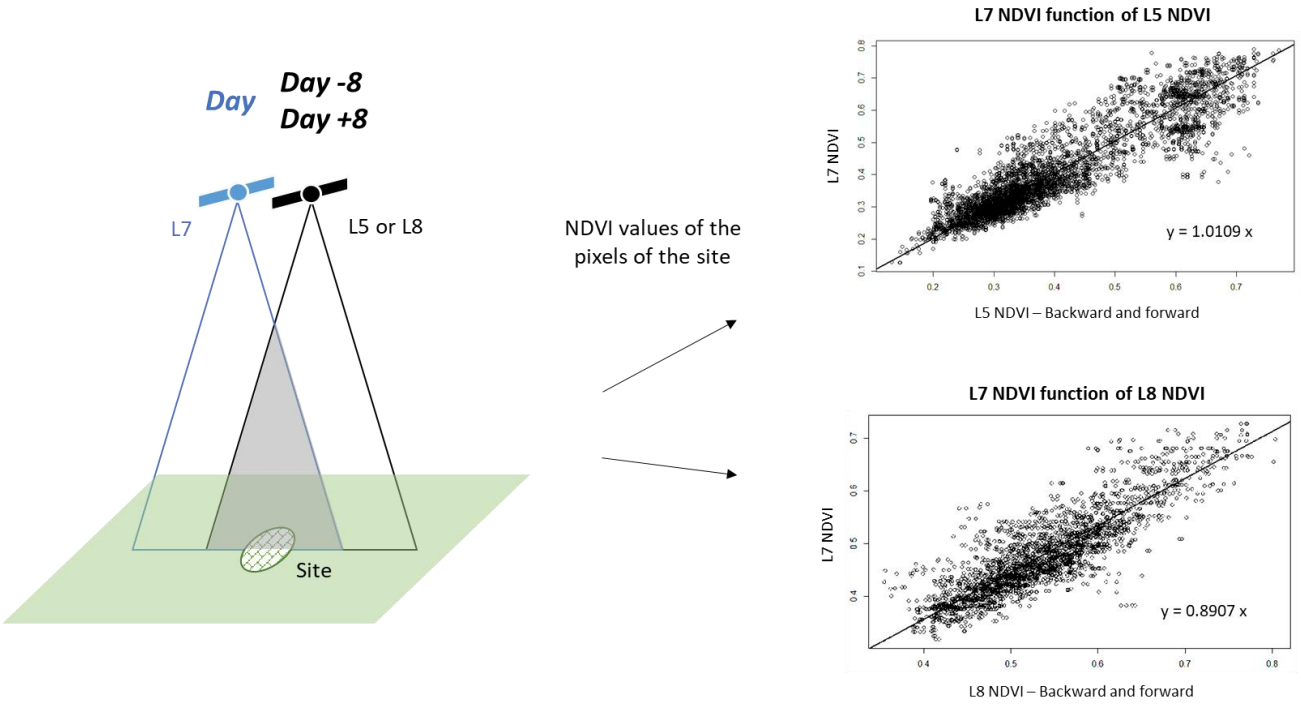

Figure 3: Methodology to adjust the NDVI values derived from different Landsat sensors.

Source: Valentine AUBARD, 2018

Table 4: Bibliographic equations of adjustment.

Reference	X	a	b
Steven *et al.*, 2003	L5	1.0210	-0.0010
Ju *et al.*, 2016	L5	1.0370	0
Roy *et al*., 2016	L8	0.9589	0.0029
She *et al.*, 2015**	L8	1.0204	-0.0112

** equation for evergreen forests NDVI in summer.

Equations are under the form Y = a * X + b, where Y is the Landsat-7 derived-NDVI and X either Landsat-5 (L5) or Landsat-7 (L7) NDVI.

Table 5: Determined site-specific NDVI adjustment equations between Landsat sensors.

Site	X	Backward images	Forward images	Total images	Available pixels	a	R^2
Bêbeda	L5	52	76	128	1165	1.0205	0.9866
Contenda	L5	17335	14212	31547	6445	1.0101	0.9754
Coruche	L5	123	124	247	1984	1.0124	0.9922
Grândola	L5	26175	21395	47570	5191	1.0109	0.9821
Lezírias	L5	65	63	128	1362	1.0039	0.9878
Portel	L5	9095	8457	17552	5863	1.0345	0.9772
Bêbeda	L8	879	888	1767	2526	0.8907	0.9931
Contenda	L8	9361	9975	19336	5904	0.8976	0.9832
Coruche	L8	145	142	287	2333	0.9050	0.9915
Grândola	L8	32856	34359	67215	5098	0.8793	0.9862
Lezírias	L8	79	78	157	1731	0.8974	0.9893
Portel	L8	10540	11387	21927	6061	0.8600	0.9841

Equations are under the form Y = a * X (considering b = 0), where Y is the Landsat-7 derived-NDVI and X either Landsat-5 (L5) or Landsat-8 (L8) NDVI. The number of images on Day -8 and Day +8 are quiet equilibrated. Less clear images are available for the sites close to the sea (frequent clouds). However, the total number of available pixels is always greater than 1000.

1.4 Months used to establish trends

One-hectare NDVI averages were extracted for each site between 1984-01-01 and 2017-12-31. Previous studies run in Machoqueira do Grou (Coruche) about the reflectance of trees, herbaceous and shrubs along years (Cerasoli *et al.*, 2016) have proven that cork oaks NDVI response was close to steady through the year, while the herbaceous absorbance shows large phenological variations, being the lowest in the driest-summer months of July and August (**Appendix 3.a**). Basically, the herbaceous vegetation dries by lack of water in summer while the trees, due to deeper root systems, access to groundwater reserves all over the year. This result is less reliable for shrubs, mainly depending on the species (**Appendix 3.b**).

To reduce understorey influence and establish the trends of each site focusing on the tree layer (cork or holm oak), only July-August mean-NDVI value was used in each year. The absence of outliers was previously checked for each plot using July-August NDVI values interquartile range (range between 25^{th} and 75^{th} percentile), to introduce no error in the mean. Focusing on summer months has also the double advantage of reducing the area of tree shadows on the images (due to high solar elevation angle) and creating an equally-distant-in-time dataset. Making the hypothesis that the trends were monotonic, the non-parametric Mann-Kendall test (Mann, 1945; Kendall, 1975) was used to obtain the strength and direction of the trends, and a value of the rate of change (slope) was given by Theil-Sen robust linear estimator (Theil, 1950; Sen, 1968). The null hypothesis of Mann-Kendall test is that there is no monotonic trend in the series, alternative hypothesis are the existence of a positive or negative monotonic trend. A Pettitt test (Pettitt, 1979) was also applied to approximate the date of a potential change-point. Those tests were run in R software using packages *stats* version 3.4.2 (R Core Team, 2017), *zyp* version 0.10-1 (Bronaugh and Werner, 2013) and *trend* version 1.1.0 (Pohlert, 2018).

1.5 Effect of precipitation and debarking on trees NDVI

Based on current knowledge and scientific literature, two variables were supposed to have a noticeable effect on NDVI variations: groundwater and debarking. As a matter of fact, one of the strategies of the tree to respond to hydric stress, e. g. caused by lack of groundwater or by debarking (traditionally made between June and August), is to regulate evapotranspiration by decreasing foliage extent (Paulo *et al.,* 2017; Mendes *et al.*, 2016; Natividade, 1950). The annual cumulated waterfall can be used as a proxy to estimate the variations of groundwater resources (Ferreira et al., 2007). A positive relation between annual precipitation rate and July-August trees NDVI is thus expected, while a negative effect of debarking could be observed. These variables were used for the definition of multiple linear regressions that were fitted using *stats* package from R software version 3.4.2 (R Core Team, 2017). Normality of distribution, absence of multicollinearity, and homoscedasticity of the dataset were checked.

The annual cumulated precipitation (cum_precip) was calculated using the nearest meteorological stations data from each study-site (**Figure 2**), available at the network SNIRH – Sistema Nacional de Informação de Recursos Hídricos (https://snirh.apambiente.pt/), from $August_{t-1}$ to $July_t$ to be coherent with $NDVI_t$, mean of $July_t$ and $August_t$ months values. The previous summer $NDVI_{t-1}$ was included in the equation, since the NDVI series is supposed to be temporally correlated (**Equation 2**). To separate the effects of the precipitation for each season of the year, a second model was tested (**Equation 3**) that includes separate variables for spring (precip_spring), summer (precip_summer), autumn (precip_autumn) and winter (precip_winter). Trees are debarked with a minimum of 9-year time-gap that is sometimes extended for 10 or 11 year's intervals. Taking advantage of the knowledge of extract

debarking years on each of the six plots considered, it was possible to test the hypothesis that the debarking operation has an impact on the NDVI of the same year or of the next year. Presence of debarking on the same year ($debark_t$) or the year before NDVI measurement ($debark_{(t-1)}$) was added in **Equation 4**.

$$NDVI_t \sim \beta_0 + \beta_1 * year_t + \beta_2 * NDVI_{(t-1)} + \beta_3 * cum\_precip + \varepsilon \quad \textbf{Equation 2}$$

where $NDVI_t$ is the annual $July_t$-$August_t$ mean of Landsat-derived NDVI, $year_t$ is the year of $NDVI_t$ measurement, $NDVI_{(t-1)}$ is the NDVI of the previous year, cum_precip is the cumulated precipitation from $August_{t-1}$ (of $year_{t-1}$) to $July_t$ (of $year_t$), β_0 is the intercept and β_1, β_2, β_3 are the correlation coefficients associated with the independent parameters and ε is the random error component.

$$NDVI_t \sim \beta_{0'} + \beta_{1'} * year_t + \beta_{2'} * NDVI_{(t-1)} + \beta_{3'} * precip\_autumn + \beta_{4'} * precip\_winter + \beta_{5'} * precip\_spring + \beta_{6'} * precip\_summer + \varepsilon' \quad \textbf{Equation 3}$$

where $NDVI_t$ is the annual $July_t$-$August_t$ mean of Landsat-derived NDVI, $year_t$ is the year of $NDVI_t$ measurement, $NDVI_{(t-1)}$ is the NDVI of the previous year, precip_autumn, precip_winter, precip_spring, precip_summer the annual cumulated precipitation per season, respectively from $September_{t-1}$ to $November_{t-1}$, $December_{t-1}$ to $February_t$, $March_t$ to May_t, $June_t$ to $August_t$, $\beta_{0'}$, the intercept and $\beta_{1'}$, …, $\beta_{6'}$ the correlation coefficients associated with the independent parameters and ε' the random error component.

$$NDVI_t \sim \beta_{0''} + \beta_{1''} * year_t + \beta_{2''} * NDVI_{(t-1)} + \beta_{3''} * cum\_precip + \beta_{4''} * debark_t + \beta_{5''} * debark_{(t-1)} + \varepsilon'' \quad \textbf{Equation 4}$$

where $NDVI_t$ is the annual $July_t$-$August_t$ mean of Landsat-derived NDVI, $year_t$ is the year of $NDVI_t$ measurement, $NDVI_{(t-1)}$ is the NDVI of the previous year, cum_precip the cumulated precipitation from $August_{(t-1)}$ to $July_t$, $debark_t$, the existence of a debarking on the same year, $debark_{(t-1)}$ the existence of a debarking on the previous year, $\beta_{0''}$, the intercept and $\beta_{1''}$, …, $\beta_{5''}$ the correlation coefficients associated with the independent parameters and ε'' the random error component.

2. Results and Discussion

2.1 Best NDVI-adjustment equations

To evaluate the performances of bibliographic and site-specific equations (respectively in **Table 4** and **Table 5**), for adjusting the three Landsat sensors NDVI values, samples were taken from the periods shared by two sensors: from 1999-01-01 to 2012-05-05 for Landsat-5 and -7 derived NDVIs; from 2013-04-11 to 2017-12-31 for Landsat-7 and -8 derived NDVIs. Since the populations do not follow a normal distribution (**Appendix 4**) and time-series observations are supposed auto-correlated, it was chosen to compare the percentages of differences between means and medians of Landsat-7 sample and the corresponding Landsat-5 and Landsat-8 samples not-adjusted and adjusted with each equation (respectively **Table 6** and **Table 7**). Boxplots were plotted for a visual approach (**Appendix 5**).

To adjust Landsat-8 NDVIs according to Landsat-7 values, no bibliographic equation fitted well. The site-specific correction is accurate enough to be used for each site. For studying a large area at a 30m-pixel scale (e.g. mainland Portugal), however, this methodology is for now too demanding in terms of processing to be applied on GEE. The simplest and safest solution is thus to not used Landsat-8 values, since Landsat-7 reaches the end of the period chosen. To adjust Landsat-5 NDVI according to Landsat-7, the observed differences seem far less important than between Landsat-8 and Landsat-7 NDVI. The equation given on the works of Ju *et al.* (2016) gives the closest values. This equation will be considered good enough to be used at small and large study areas.

2.2 Evolution of NDVI values along years

Landsat-5 and Landsat-8 had been adjusted for each site with its specific equation. Not-adjusted NDVI values of Landsat-8 are always greater than Landsat-7 values on equivalent dates, while Landsat-5 values are always lower. Adjusted values are similar to Landsat-7 NDVI for the same period (**Appendix 6**)**.** The evolution of NDVI values have been compared graphically between Landsat and MODIS sensors (**Figure 4**). The values are close and their evolution is identical along years. Every plot presents a large intra-annual variation of NDVI due to vegetation phenology. The maximum are reached in December-January and the minimum in July-August. The difference between those two values depends of the percentage of canopy cover (Häusler *et al*., 2016). Those observations support the hypothesis that NDVI cycles exist for every composition of understorey and every percentage of canopy cover.

2.3 Explaining NDVI variations with precipitation and debarking

Fitting the multilinear regression with all of the stands simultaneously decrease the effect of the variable $year_t$ (**Equation 2**, **Table 8**) and lets appear the high correlation between NDVI values of one year and the next ($NDVI_{t-1}$ and $NDVI_t$). As expected, annual precipitation amounts are positively correlated to NDVI values: more precipitation, higher NDVI. The works of Caritat *et al*. (2000) and Faias *et al*. (2018) already showed annual cork rings thickness is positively correlated with annual precipitation. These results thus confirm NDVI is a good proxy for following cork oaks (cork) productivity. $Year_t$, being a significant component, suggests other variables are needed to fully explain NDVI values, such as other pedo-climatological variables or human practices (debarking, shrubs management, grazing).

Table 6: Percentages of absolute differences in means (%D means) and medians (%D medians) between Landsat-5 and Landsat-7 NDVI.

Site	Type	L5 Raw Data	L5 Steven *et al.*, 2003	L5 Ju *et al.*, 2016	L5 Site specific
Bêbeda	%D means	-5.275	-3.492	-1.770	-3.329
Contenda	%D means	-8.785	-7.085	-5.410	-7.868
Coruche	%D means	-3.499	-1.644	0.072	-2.303
Grândola	%D means	-9.750	-8.074	-6.411	-8.764
Lezírias	% Dmeans	-1.707	0.177	1.930	-1.324
Portel	% Dmeans	-7.582	-5.880	-4.162	-4.391
Average mean error (%)		-6.099	-4.392	-3.292	-4.663
Bêbeda	%D medians	-5.010	-3.224	-1.496	-3.060
Contenda	%D medians	-13.134	-11.540	-9.920	-12.260
Coruche	%D medians	-3.293	-1.435	0.285	-2.094
Grândola	%D medians	-10.412	-8.772	-7.097	-9.433
Lezírias	%D medians	-1.815	0.066	1.818	-1.432
Portel	%D medians	-6.667	-4.963	-3.213	-3.444
Average median error (%)		-6.722	-5.000	-3.971	-5.287

Table 7: Percentages of absolute differences in means (%D means) and medians (%D medians) between Landsat-8 and Landsat-7 NDVI.

Site	Type	L8 Raw Data	L8 Roy *et al.*, 2016	L8 She *et al.*, 2015	L8 Site specific
Bêbeda	%D means	12.874	8.839	12.843	0.539
Contenda	%D means	11.640	7.707	11.385	0.207
Coruche	%D means	9.218	5.207	9.602	1.159
Grândola	%D means	12.712	8.689	12.659	0.888
Lezírias	%D means	9.452	5.437	9.819	1.783
Portel	%D means	19.949	15.789	19.422	3.156
Average mean error (%)		12.641	8.611	12.622	1.289
Bêbeda	%D medians	14.681	10.584	14.637	2.148
Contenda	%D medians	13.299	9.384	12.746	1.696
Coruche	%D medians	9.885	5.846	10.281	0.555
Grândola	%D medians	17.209	13.066	16.996	3.066
Lezírias	%D medians	9.983	5.946	10.363	1.306
Portel	%D medians	24.588	20.337	23.771	7.145
Average median error (%)		14.941	10.861	14.799	2.653

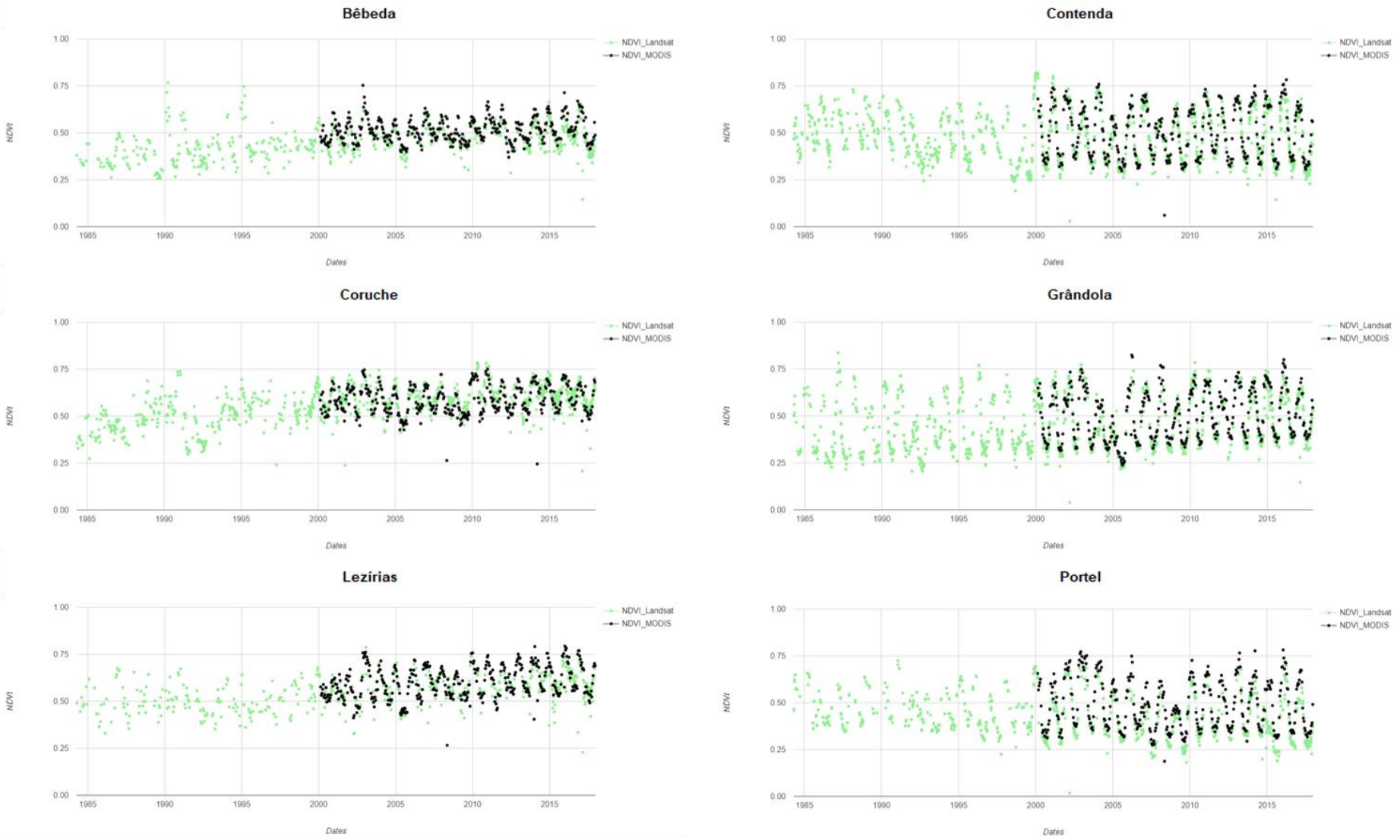

Figure 4: Comparison of adjusted-Landsat and MODIS NDVI variation along years.

In the second model (**Equation 3**), where cumulated precipitation is decomposed per seasons, adjusted-R-squared is slightly better (**Table 9**). Precip_autumn and precip_winter are not significantly explaining NDVI values of July-August, there is supposedly no hydric stress on those seasons. Of course, it can also be a bias from taking only summer NDVI values. The main impacts on NDVI are found in spring, when the these oaks produce new leaves, and in summer, when the temperatures cause an important need of water, making the trees very sensible to the variations of precipitation during this season. These results are in line with the ones obtained by Caritat *et al*. (2000). It is also in June and July than cork oaks produce the most quantity of cork under favourable climate conditions (Costa *et al*., 2003). One of the tree's strategies in case of hydric stress is to lower transpiration by losing leaves, which will therefore decrease NDVI values, allowing to follow health and productivity.

Debarking of $year_t$ has no significant effect on summer $NDVI_t$ (**Equation 4, Table 10**). A possible explanation for this is that since the cork is removed between June and August (**Table 2**), when the new leaves of the year are already well developed, the operation will not have an important impact on the NDVI values recorded. Supporting this result is the fact that a minor effect of the debarking in the leaves may be observed, in some trees, during a short and varying period of time averaging 15 days after debarking, when the trees are recovering from loss of water by transpiration of the stem (Natividade, 1950; Correia *et al.*, 1992; and Werner and Correia, 1996), which is a too short reaction to be observed by a 2-month-mean of NDVI.

Results also show a significant negative effect of the debarking ($debark_{t-1}$) on next year $NDVI_t$. An hypothesis would thus be that the trees, in the spring after the debarking operation, allocate resources and photo-assimilated compounds to produce a new cork layer that allows to increase the protection from fire and loss of water during summer, delaying and/or decreasing leaf production to a later season such as autumn or even to the following year. This hypothesis is supported by the observations of Vaz *et al.* (2010) or Costa e Silva *et al.* (2015), that observed this event respectively after a dry summer and a dry winter.

2.4 Significant NDVI trends for the six study-sites

The **Table 11** below presents the results for the Pearson's correlation and the Mann-Kendall test, using the annual means of July-August Landsat-5 adjusted, -7 and -8 adjusted-derived NDVI. Pearson's null hypothesis is that there is no correlation in the population, and its alternative hypothesis is that there is correlation (here, between NDVI values and the time in years). Its results is between -1 and 1, with 1 being a total positive correlation, 0 an absence of correlation and -1 being a total negative correlation. The significance of the correlation is given by a two-sided p-value and the limits of its confidence interval (conf. Int.). Mann-Kendall test is non-parametric and resistant to outliers, gives the significance and sign of a supposed monotonic trend in a time series (here July-August NDVI values for 34 years). The sign of its result, *tau*, indicates the sign of the trend. *Tau* has a value between -1 and 1, which follows a normal distribution for times series longer than 30 years, so the value can be used directly to determine the significance of the trend (values between -1.96 and 1.96). Its two-sided p-value give the same result.

For Landsat, the Pearson's confidence intervals show how far from 0 all the correlations are. The p-values, similar for Pearson and Mann-Kendall tests, are highly significant, asserting the existence of strongly significant trends for each site. The sign of Pearson's correlation and Kendall's *tau* match. Two study-sites, Contenda and Portel, have a decreasing trend of NDVI between 1984 and 2017. They are actually the two plots with lower cork production per tree (**Table 1**). The other stands present a positive trend.

Table 8: Parameter estimates for the $NDVI_t$ model (Equation 2).

	Estimate	Std. Error	t-value	p-value
Intercept	-1.716e+00	8.482e-01	-2.023	0.04447
$year_t$	8.694e-04	4.222e-04	2.059	0.04081
$NDVI_{(t-1)}$	8.697e-01	3.758e-02	23.141	< 2e-16
cum_precip	5.562e-05	1.705e-05	3.261	0.00131

Multiple R-squared: 0.7396 Adjusted R-squared: 0.7356.

Table 9: Parameter estimates for the $NDVI_t$ model (Equation 3).

	Estimate	Std. Error	t-value	p-value
Intercept	-2.191e+00	8.179e-01	-2.679	0.008029
$year_t$	1.098e-03	4.072e-04	2.698	0.007607
$NDVI_{(t-1)}$	8.854e-01	3.606e-02	24.554	<2e-16
precip_autumn	-2.584e-05	3.320e-05	-0.778	0.437469
precip_winter	4.467e-05	2.690e-05	1.660	0.098518
precip_spring	1.955e-04	5.218e-05	3.746	0.000238
precip_summer	4.919e-04	1.184e-04	4.153	4.94e-05

Multiple R-squared: 0.769 Adjusted R-squared: 0.7617

Table 10: Parameter estimates for the $NDVI_t$ model (Equation 4).

	Estimate	Std. Error	t-value	p-value
Intercept	-1.850e+00	8.790e-01	-2.104	0.036643
$year_t$	9.347e-04	4.375e-04	2.137	0.033892
$NDVI_{(t-1)}$	8.776e-01	3.739e-02	23.468	<2e-16
cum_precip	6.160e-05	1.763e-05	3.494	0.000591
$debark_t$	5.035e-03	1.282e-02	0.393	0.695008
$debark_{(t-1)}$	-2.575e-02	1.109e-02	-2.322	0.021263

Multiple R-squared: 0.747 Adjusted R-squared: 0.741

Table 11 : Pearson's correlation and Mann-Kendall Tau.
The non-significant p-values are in red.

Site	Sensor	Pearson's correlation	Pearson's conf. Int. 1	Pearson's conf. Int. 2	Pearson's p-value	Kendall's tau	Kendall's p-value
Bêbeda	Landsat	0.6929	0.4633	0.8353	5.5778E-06	0.4795	3.6492E-05
Contenda	Landsat	-0.6521	-0.8113	-0.4027	2.9383E-05	-0.4118	4.7160E-04
Coruche	Landsat	0.8010	0.6348	0.8964	1.2721E-08	0.6506	3.7796E-09
Grândola	Landsat	0.6061	0.3371	0.7837	1.4503E-04	0.5009	1.4614E-05
Lezírias	Landsat	0.7820	0.6034	0.8859	4.7220E-08	0.5911	9.2024E-07
Portel	Landsat	-0.7717	-0.8815	-0.5828	1.4590E-07	-0.5909	2.5609E-07
Bêbeda	MODIS	0.0639	-0.4154	0.5154	8.0113E-01	0.0327	8.8135E-01
Contenda	MODIS	-0.0717	-0.5212	0.4088	7.7724E-01	-0.0525	7.6171E-01
Coruche	MODIS	0.2749	-0.2202	0.6574	2.6960E-01	0.1242	5.0087E-01
Grândola	MODIS	0.6688	0.2936	0.8655	2.4063E-03	0.5948	3.2463E-04
Lezírias	MODIS	0.5981	0.1820	0.8325	8.7512E-03	0.4459	9.9508E-03
Portel	MODIS	-0.1864	-0.6010	0.3072	4.5887E-01	-0.2288	2.0082E-01

A negative trend of NDVI for a cork oak stand can be easily interpreted: either some trees are already dead and thus removed, originating more open stands; either the trees are not healthy and didn't produce new leaves in May-June as usual. Those two reasons, cumulated or not, have obvious consequences on the global yield of the stand. On the other hand, an increasing NDVI is expected in a healthy stand, since the trees are supposed to grow, and their canopy cover is supposed to extend each year. Grândola and Lezírias significant MODIS p-values have signs similar to the Landsat ones, thus confirming them. The other stands have non-significant p-values (in red in **Table 11**), their confidence intervals surround 0. Either the time series of 18 years is not long enough for any trend to be significant, either there is an absence of trend during MODIS period for those stands. To explore this last possibility, a test of Pettitt has been made on Landsat dataset to test the existence of a change-point in the trends.

2.5 Rate of change of the trends

The trend slope was established with the Theil-Sen estimator, a robust to outliers and non-parametric statistic method fitting a line in the plane. A graphic result per plot can be observed on **Figure 6**. A classic linear regression associated to a t-test on the linear coefficients were also calculated to compare results. The null hypothesis of the t-test is that no linear relationship exist between X and Y (here the time in years and NDVI values), the alternative hypothesis is the existence of a linear relation.

The intercept (b) and slope (a) of the linear regression and Theil Sen estimator are very close (**Table 12**). The signs are the ones announced by the test of Mann-Kendall. The minimal slope can be found for Portel, with a decrease of 0.0048 units per year. The highest increase of NDVI is for Coruche, where a_{TS} = 0.0061 for the period 1984 – 2017. The graphic of the Theil-Sen 34-year NDVI trends against the mean cork production (presented in **Table 1**) suggests a linear or exponential relation between those two variables (**Figure 5**), although this study would need to be extended to more sites to give strengthen these conclusions.

Table 12: Linear trend (L) and Theil Sen estimator (TS) comparison.

Site	a_L	b_L	p-value$_L$	a_{TS}	b_{TS}
Bêbeda	0.0036	-6.7690	5.5778E-06	0.0035	-6.6673
Contenda	-0.0037	7.6685	2.9383E-05	-0.0035	7.3442
Coruche	0.0066	-12.6089	1.2721E-08	0.0061	-11.6559
Grândola	0.0023	-4.2797	1.4503E-04	0.0024	-4.3825
Lezírias	0.0045	-8.4146	4.7220E-08	0.0045	-8.4130
Portel	-0.0054	11.1970	5.1979E-08	-0.0048	9.9479

*Relations are under the form: NDVI = a * Year + b.*

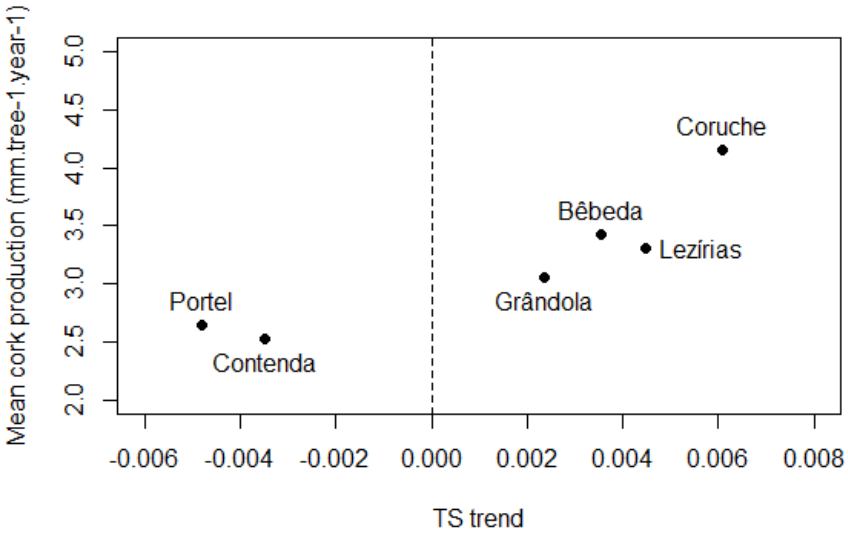

Figure 5: Mean cork production in millimetres per year per plot function of 34-year NDVI trends (from 1984 to 2017).

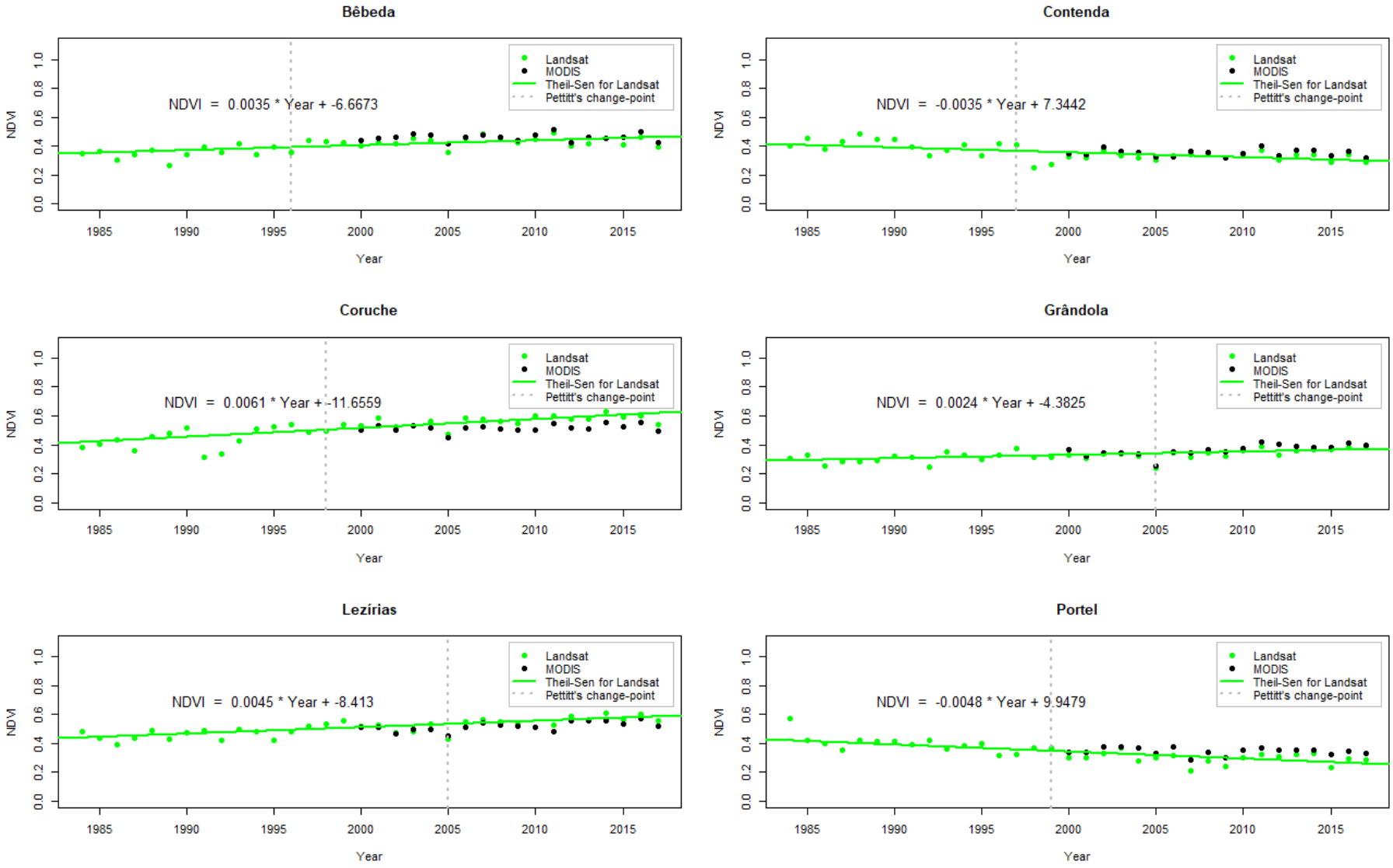

Figure 6: Landsat NDVI summer means per year for each study-site.

2.6 Trend change-point

The non-parametric test of Pettitt's null hypothesis is that there is no change-point in the series, while its alternative hypothesis is that a change-point exists. It gives the time K (here, on a total of 34 years) at which there is probably a change-point in the trend. The result is considered significant if the p-value is lower than 0.05. The **Table 13** resumes the results for the Landsat NDVIs means of summer months, for each site-study. Trends change-points are indicated by vertical dotted lines on **Figure 6**.

Table 13: Results of Pettitt change-point test per study-site for Landsat time-series (1984- 2017).

Site	Pettitt's K	Year of change-point	Pettitt's p-value
Bêbeda	13	1996	2.0321E-04
Contenda	14	1997	3.9029E-04
Coruche	15	1998	9.5670E-05
Grândola	22	2005	9.4637E-03
Lezírias	22	2005	4.4973E-04
Portel	16	1999	7.5878E-05

Four stands seem to have a significant change of trend in the late 20th century. This could correspond to the use of a new sensor, Landsat-7, after 1999, giving different values of NDVI. A non-perfect equation of adjustment between the sensors could cause such results. However, Lezírias and Grândola have a significant change point later, probably in 2005. They are the two plots for which MODIS trends were significant with both Pearson and Mann-Kendall tests. In this case, it could mean an acceleration of change rate after 2005, increasing the trend significance and making it detectable even with MODIS short time series. Change-points can also be explained by an evolution more polynomial than linear of the NDVI, caused by biological factors like the age of the trees, or by changes of trends in other processes, like temperature and precipitation in a context of abrupt climate change.

3. Conclusion of Part 1

This first study was not exhaustive, and more plots would be needed to refine results. It would be interesting to make this analysis using other vegetation indices, like the Enhanced Vegetation Index, which is less sensitive to understorey. Nevertheless, NDVI seems to be a good proxy for productivity of cork oak stands, as first results suggest a relation between NDVI trends and cork growth. For last, future studies will allow to improve the understanding of precipitation and debarking impacts and enlarge the dataset in space and time.

For a study in all continental territory of Portugal, the imperfect adjustment between Landsat-derived NDVIs does not allow the use of Landsat-8 values for the time being. Landsat-5 and -7 -derived-NDVIs can be used with confidence, considering their values and evolution had been validated by MODIS values. The hypothesis of monotonic trends of NDVI can be maintain, since Mann-Kendall test revealed to be significant for all plots and consistent with TS slope signs. Relations between trends of dependent and independent variables need to be explored to clarify change-points detected by Pettitt test.

Part 2: Mapping NDVI trends for continental Portugal

The objective of this second part was to map NDVI trends for all areas covered by the dominant oak species in continental Portugal, cork oak (*Quercus suber L.*) and holm oak (*Quercus ilex L.*).

4. Material and methods

4.1 Selected areas

To determine the spatial distribution of the species studied, the Land Use and Land Cover Map of Portugal (*Carta de Uso e Ocupação do Solo* (COS); maps and technical documents can be found on the webpage http://www.dgterritorio.pt/dados_abertos/cos/) was the most precise in spatial scale and classification. It characterises homogeneous areas with at least 1 hectare and 5-level hierarchical classification with 193 classes for the fifth level. It is currently available for 1995, 2007, 2010 and 2015. Five classes were chosen to summarise the COS, extracting cork and holm oak forestry and agro-forestry systems (**Table 14**). **Appendix 7**Appendix 8 presents matches between each COS classes (in Portuguese) and the code of the classes kept.

Only the areas with a constant land cover class, i.e. where class transitions were not observed in the period 1995-2015, were considered in the trend analysis (**Figure 7, left**; enlargement of the map can be found on **Appendix 9.a**). A complete comparison of the area covered per each land cover class per COS and the areas of constant class can be found on **Appendix 8**.

A mask of burned areas (**Figure 7, right**; enlargement of the map can be found on **Appendix 9.b**) between 1984 and 2017 was applied, in order to exclude from the analysis burned stands repopulated with the same species, thus appearing to be of constant cover class within the COS but would present irrelevant NDVI evolution.

4.2 Images, NDVI and time series

According to what has been previously exposed in Part 1 (2.1), only Landsat-5 and -7 already corrected images from GEE were used to established trends at 30-meter spatial resolution from 1984 to 2017 for the areas of Portugal covered with oak species. A *Fmask* ensures to mask clouds and shadows. Only results for NDVI, the most common vegetation index, will be presented. Landsat-5-derivated NDVI values (X) has been adjusted to Landsat-7-NDVIs (Y) following the linear relation $Y = 1.0370 * X$ of Ju *et al.* (2016). Like before, but this time per pixel, only annual mean of NDVI values of July and August were extracted from GEE, in order to avoid understorey noise and get an evenly-spaced in time series. In IDRISI 17.0 Selva Edition, the 34-image time series with the mean annual NDVI were then pre-whitened using Durbin-Watson residuals series pre-process of the Earth trends Modeler. The non-parametric test of Mann-Kendall, Theil Sen robust estimator and the Contextual Mann-Kendall significance test, taking into account the values of the 1st order neighbours, were then run.

Table 14: Five classes used to summarise the classification of the COS.

Code	Composition	Area (ha)
1	Cork oak forests	844153
2	Holm oak forests	264896
3	Cork oak agroforestry systems	292334
4	Holm oak agroforestry systems	614577
5	Cork and holm oak agroforestry systems	161158
-	Total	2177117

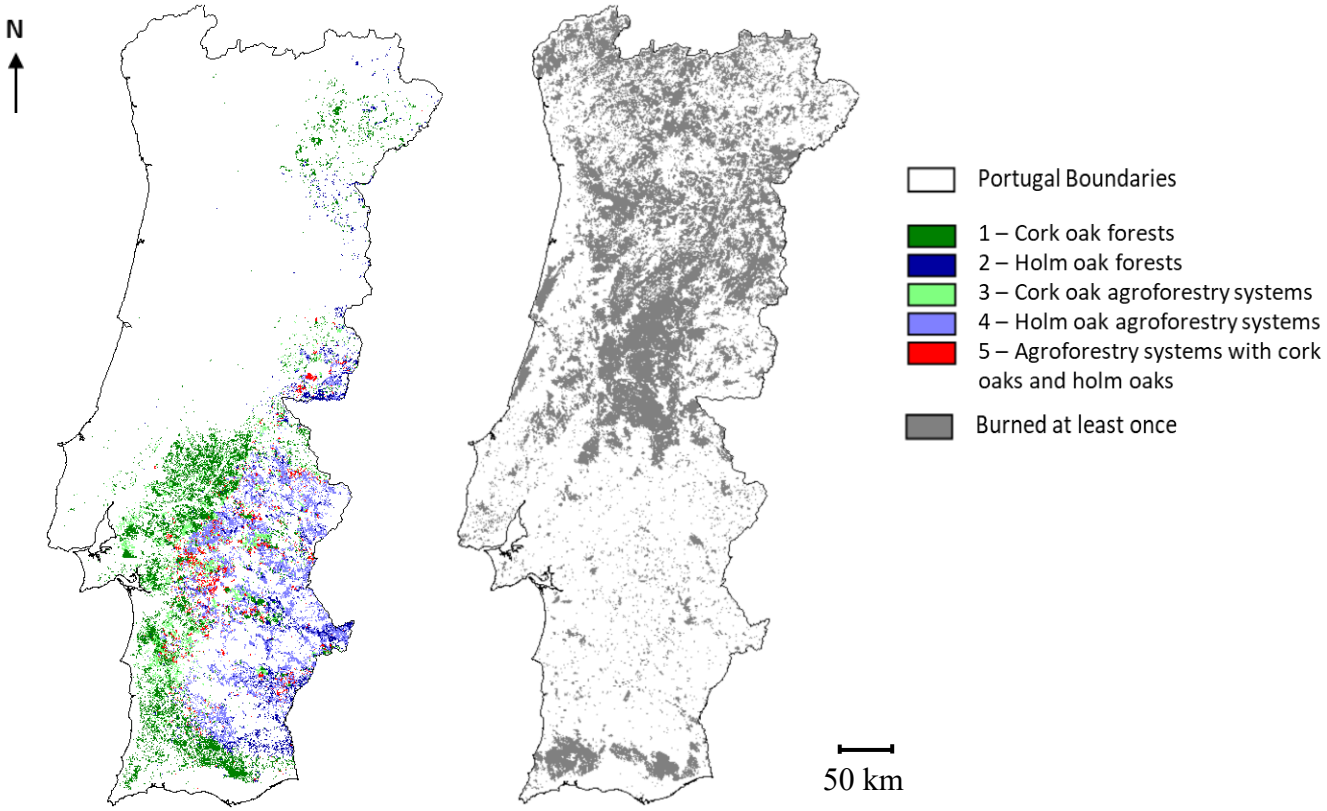

Figure 7: Masks of constant land cover classes (left) and burned areas (right).
Left: cork oak and holm oak constant areas in Portugal (1995 - 2015), from Land Use and Land Cover Maps of Portugal of 1995, 2007, 2010 and 2015. Pixel size: 30m². Minimum map unit: 1 ha.
Right: burned areas in continental Portugal (1984 and 2017), from annual burned areas maps of the Nature and Forests Conservation Portuguese Institute (Instituto da Conservação da Natureza e das Florestas, ICNF). Pixel size: 30m². Minimum map unit: 5 ha.

5. Results and Discussion

5.1 Mann-Kendall for all cork oak and holm oak woodlands in Portugal

The **Figure 8** presents the results of the Mann-Kendall test for all cork and holm oaks areas. Each pixel represents 30m-scaled on the ground. Are given significant and not significant monotonic trends and their sign. The **Table 15** following resumes the main characteristics of the results of this map.

Frequently, trends are too close to zero to be significant. With the Mann-Kendall test, not significant trends are usually isolated pixels or pixels on the border of the stands, meaning the pixel can include roads, other crop fields or water, which deform the NDVI values and its evolution. The percentage of positive trends is higher than the percentage of negative trends, for significant and not significant trends. Most of the Portuguese cork and holm oak woodlands are not decreasing in wealth or productivity. Nevertheless, 30.82% of the areas with significant trends are negative, meaning that one third of the areas may be in decline.

Table 15: Area and percentage of total area of Mann-Kendall map results.

	Area (Ha)	**Percentage of total area (%)**
Total area (firemasked)	1748300	100
Significant trends	693898	39.69
Not significant trends	1054402	60.31
Positive significant trends	482987	27.63
Positive not significant trends	612698	35.05
Negative significant trends	210911	12.06
Negative not significant trends	441703	25.26

5.2 Theil Sen slope for all Portugal

The map in **Figure 10** gives Theil-Sen magnitude of change where trends have been found significant in the previous Mann-Kendall test. It shows the main negative trends are in the region Centro, and in littoral and interior parts of the Alentejo, which can be due to climate, but also soil texture and lithology (Paulo *et al.*, 2015b). The distribution of the values of the slopes is close to normal using significant and not significant trends (**Figure 9, left**). For significant only, by construction, there is a gap in the distribution of values, since the slopes near to zero can't be considered significant (**Figure 9, right**). The distribution is slightly different from class to class (**Appendix 11**), but the mean (**Table 16**) is always in the not significant interval. The percentage of areas with a significant slope better or worse than the average corresponds exactly to the percentage given in **Table 15** respectively for positive and negative trends.

No test was done here to try to explain the spatial distribution of trends, due to a lack of available data for all Portugal for the moment. Linear models in Part 1 (2.3) already proved the importance of cumulated precipitation and debarking. To those ones can be added other ecologic (pedoclimatic, pest and diseases), biologic (age of trees, genetic, presence of natural or artificial regeneration) or anthropic factors (practices, mainly debarking, grazing and shrubs management).

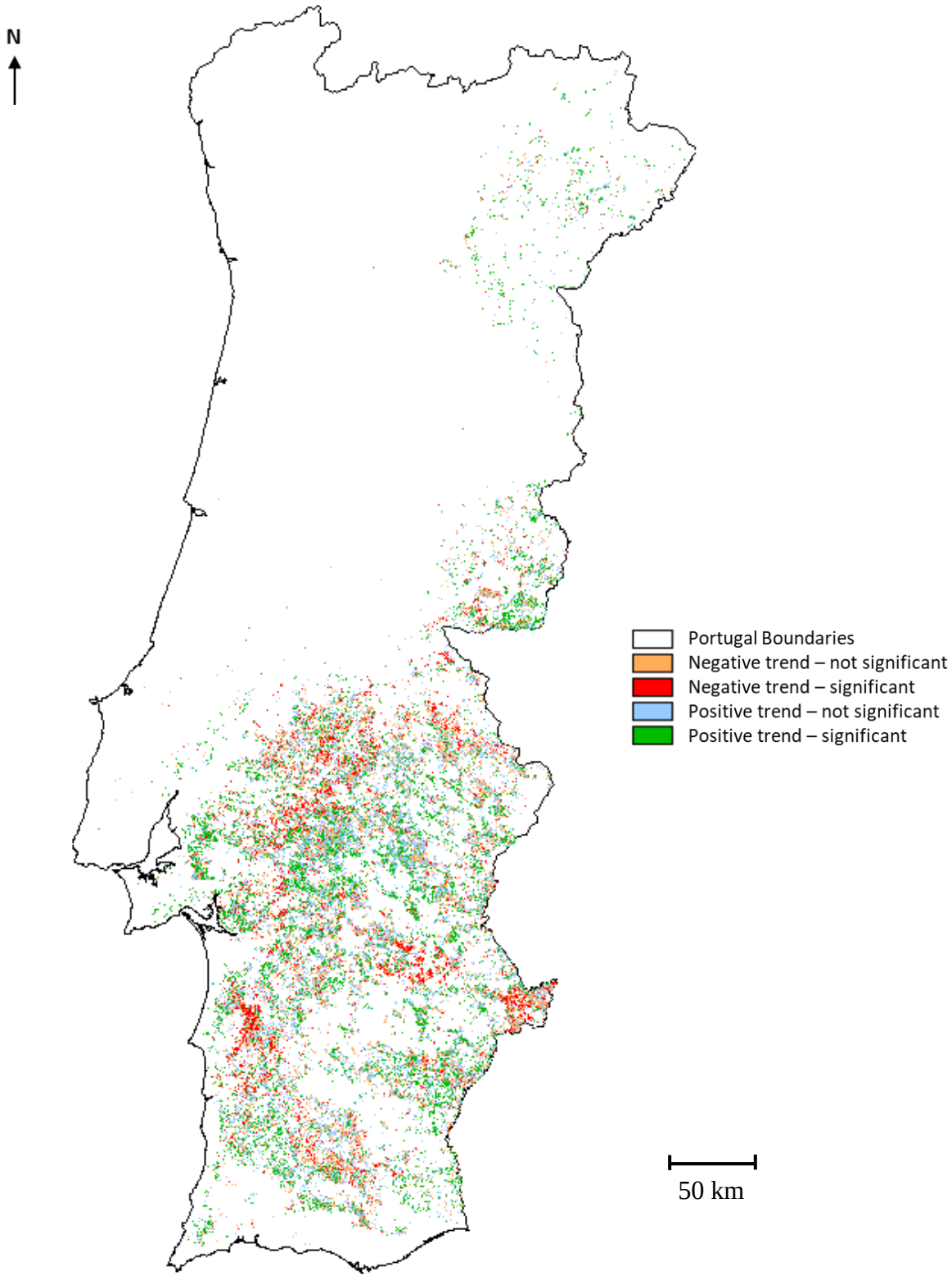

Figure 8: Mann-Kendall test results - signs and significance.

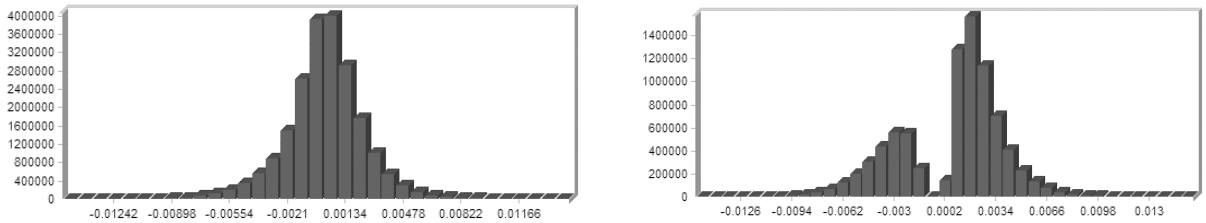

Figure 9: Frequency histogram of significant and not significant slope (left), and significant slopes only (right), for the 5 classes of land use.

Table 16: Means of Theil-Sen slope per class.

Class	Mean
All classes	0.000502
1. Cork oak forests	0.000420
2. Holm oak forests	0.000503
3. Cork oak agroforestry systems	0.000104
4. Holm oak agroforestry systems	0.000346
5. Agroforestry systems with cork oak and holm oak	0.000170

This resulting map can be discussed. First the minimal map units of the COS and fire mask are respectively of 1 hectare and 5 hectares, so the final maps ignored smaller areas, even with 30-m-squared NDVI pixels precision. It was also assumed the land cover class of the selected areas didn't change during the first 10 years of the time series, considering the stands covered by cork and holm oaks are very stable over time, due to their type and potential lifetime of exploitation, and since those protected species can't be cut without formal permission, according to the current national legislation in Portugal. Moreover, the surface that changed within the COS are in the large majority of cases only evolving between a forest and an agroforest system of the same species. Anyway, no COS exists before 1995 to guaranty that the land cover remained constant between 1984 and 1995. Then, the values of NDVI images used to establish the time series are means of two summer months, but the dates available each year does not insure the NDVI means reflect the same time range. No perfect adjustment was made between NDVI values of Landsat-5 and -7, which might have biased trends significance or its rate of change. At last, some shrubs remain green in summer, thus, at more precise scales, this kind of analysis should take into account the composition of the understorey and the percentage of canopy cover.

5.3 Mann-Kendall and Theil-Sen results per class of land cover

Percentage of significant and not significant areas and their signs were compared per class (**Table 17**). The maps specific to each class can be found in **Figure 11** (enlargements of each map is given on **Appendix 10**). The highest percentage of negative significant trends is found for cork oak agroforestry systems (3) and the lower is for holm oaks agroforestry systems (4). This difference can be explained by a better adaptability of holm oaks to xerophytic climatic conditions (David *et al.,* 2007 ; Vaz *et al.*, 2010), especially in agroforestry systems, where the low tree density and cover don't allow an efficient water retention in summer (Joffre *et al*., 1993 ; Gouveia *et al.,* 2008).

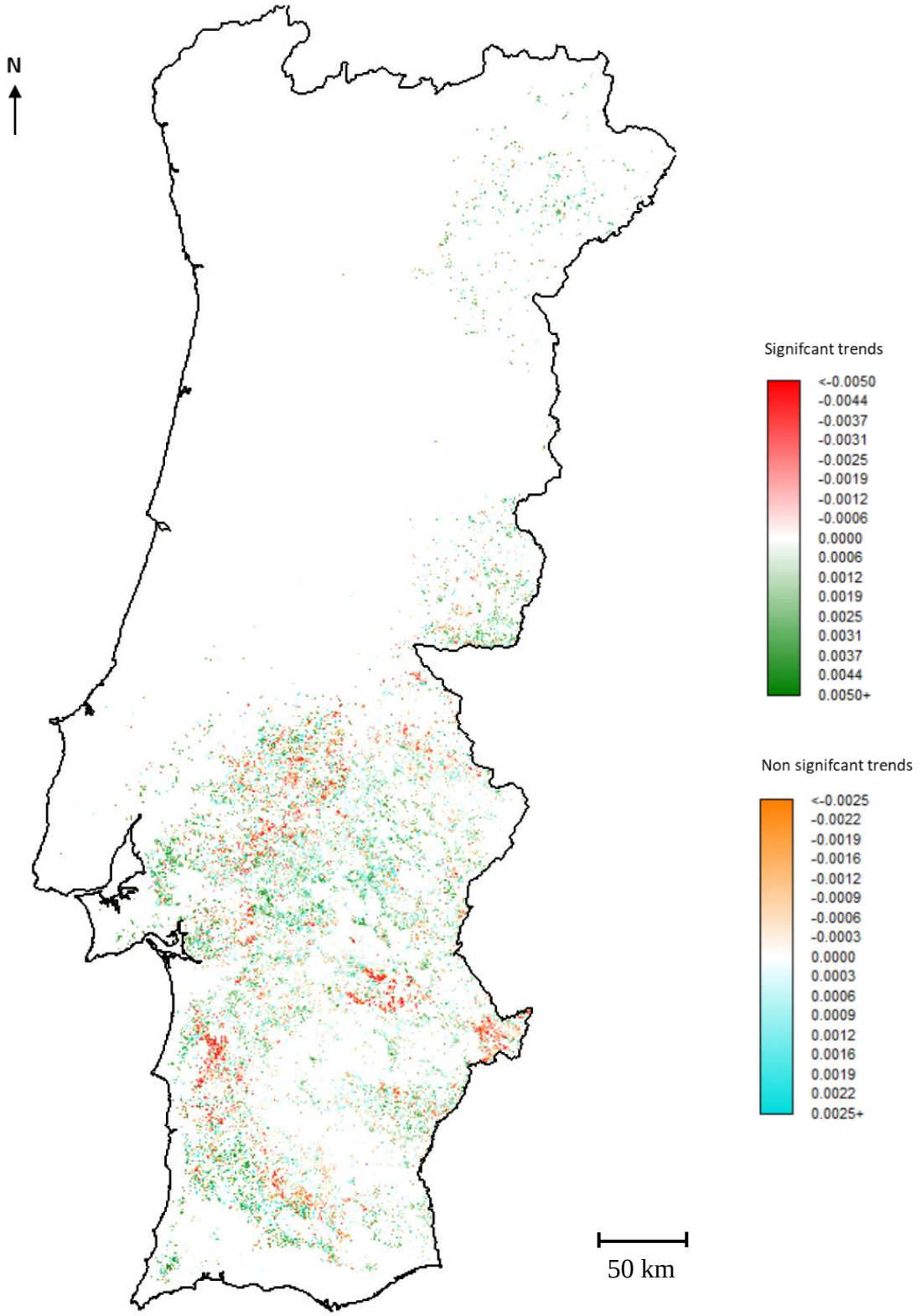

Figure 10: Theil-Sen slopes and Mann-Kendall significance.

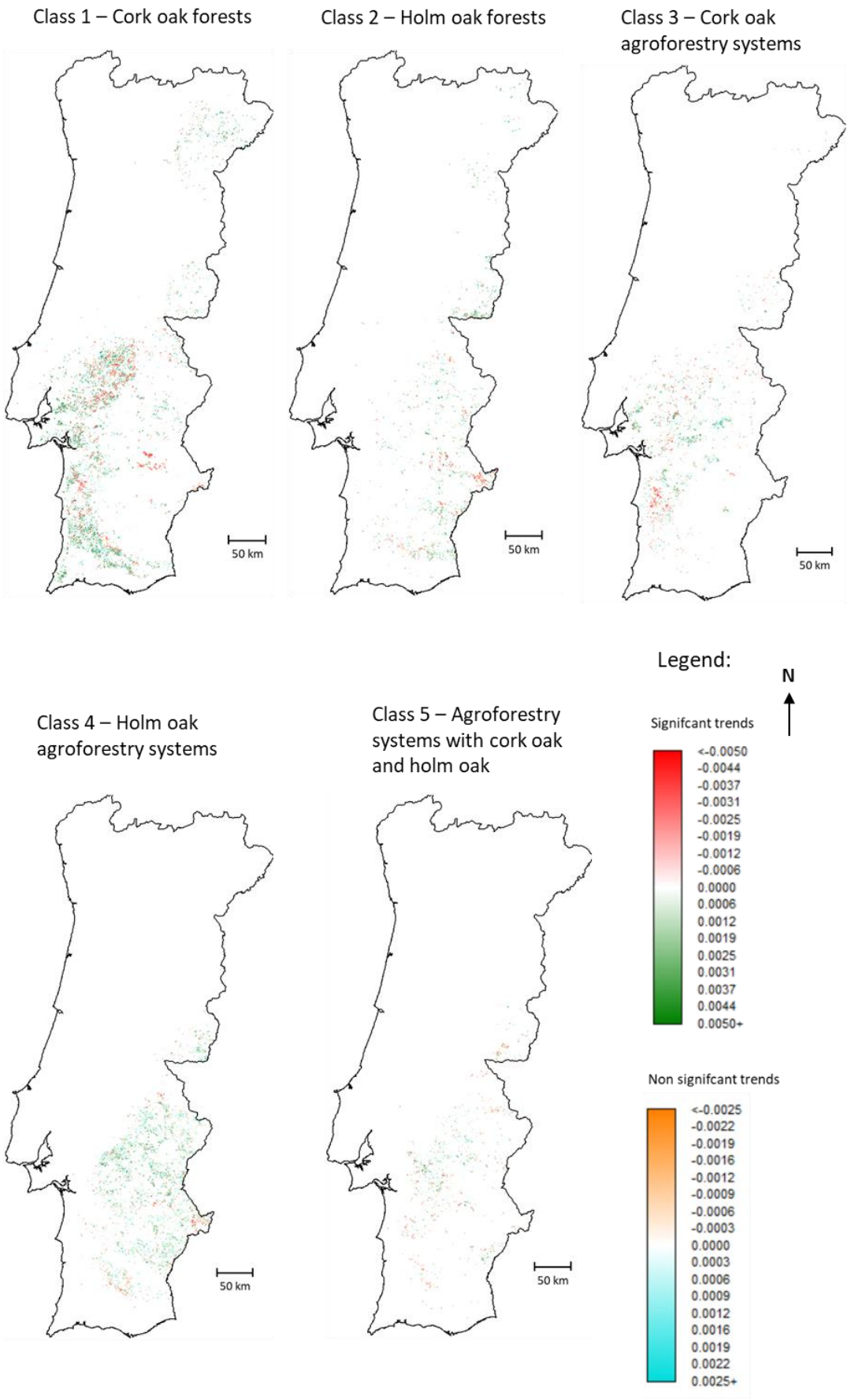

Figure 11: Theil Sen slopes and Mann-Kendall significance maps per land cover class.

Table 17: Percentage of significant and positive trends per land cover class.

Class	1	2	3	4	5
Significant trends (% of total area of the class)	41.94	45.20	40.77	34.52	35.01
Not significant trends (% of total area of the class)	58.06	54.80	59.23	65.48	64.99
Positive trends (% of significant trends)	67.88	73.09	58.85	76.14	63.72
Negative trends (% of significant trends)	32.12	26.91	41.15	23.86	36.28

1: Cork oak forests, 2: Holm oak forests, 3: Cork oak Agroforestry systems, 4: Holm oak agroforestry systems, 5: Agroforestry systems with cork and holm oak

5.4 Application to the study-sites and Contextual Mann-Kendall

The Contextual Mann-Kendall test (CMK), due to being a very long and heavy process to compute with Idrisi (temporary files proportional to the number of years, at 30m-squared, for all Portugal) was not made for the whole Portugal area. Nevertheless, enlargements of the final Theil-Sen map have been made in order to compare Part 1 and Part 2 trends results, and to show the interest of the CMK significance test for higher resolutions. **Figure 12** gives an idea of the result a CMK for all Portugal could allow: globally the same significant trends, with more significant pixels on the borders and less significant pixels isolated.

All the pixel slopes inside study-sites areas are significant, except in Grândola, where 2 pixels on 20 are not, and for the site of Portel, which is outside of the consistent area selected for the final map. This stand may have change of class in the last COS, since it has a very low canopy cover, or it is a consequence of the COS minimal units of 1 hectare, ignoring smaller areas. Anyway, the values of NDVI trends around this site of Portel are coherent with the ones found in Part 1. The rate of change of every plot correspond to the previous results (Part 1, 2.5 and **Table 12**). It is interesting to notice the spatial correlation but also the variability that can exist around each stand. In Coruche, for example, the evolution of the NDVI is very contrasting. Strong positive slopes become negative at a distance of 500 meters. An *in situ* analysis and the use of various data about the study-area (like management, field slope, exposition (Costa et al., 2010)) would help to understand this important variability.

6. Conclusion of Part 2

Two maps of all cork and holm oaks stable areas of Portugal were established, showing Mann-Kendall signs and significance and Theil-Sen estimator of linear regression of summer NDVI trends, at 30-m-squared resolution. In conclusion, one third of those woodlands are in decline according to this analysis. No possible comparison with the last centuries trends can be reasonably made, but considering regeneration should maintain woodlands in time, this result is interpreted like an alert signal of the health of the Portuguese stands and their regeneration capacity, which happens to be already one important source of discussion nowadays. More studies on this subject are needed to identify the reasons for those decreasing trends, their consequence and possible solutions.

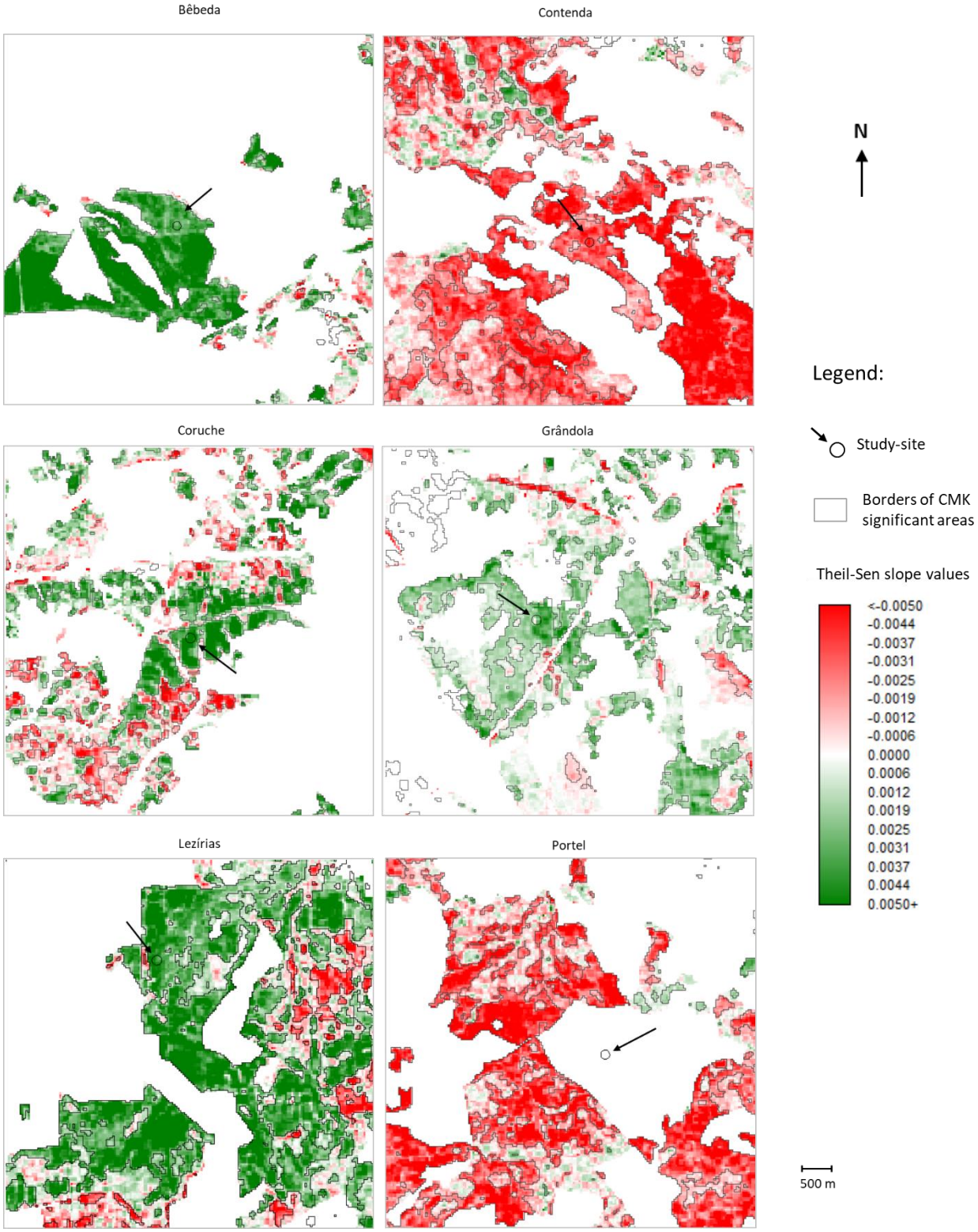

Figure 12: Theil-Sen slopes around the six study-sites, with Mann-Kendall and Contextual Mann-Kendall significance.

Slope for significant and not significant trends. Significant Contextual Mann-Kendal (CMK) areas are bordered by a grey line. Each pixel represents 30-m-squared.

General Conclusion

This work permits to point out the advantages of Google Earth Engine in order to study long time series: a fast and easy acquiring of images, construction of features and first treatments (cloud mask), data extraction (calculation of NDVI), first graphics and pixel value extraction. Nevertheless, it remains limited to run specific tests (Mann-Kendall and Theil-Sen), to extract heavy images or print huge graphics. Google Earth Engine does not replace other tools but allows a free download of data to complete the analysis outside of the platform.

Its potential was used with success in this study. In Part 1, a methodology to map 30-year-trends of NDVI of cork oaks woodlands at a resolution of 30-m-squared was established, applied to six study-sites in Portugal and validated. It was also the occasion to find explanatory variables, a relation between trends and productivity, and change-points in trends around the end of the 20th century. In Part 2, this methodology was applied to map all Portugal consistent woodlands of cork oaks and holm oaks, proving thirty percent of the total area is declining. This method can be reproduced, improved and adapted to other indices, areas and species. The resulting map is the first step to identify the reasons of this decline and anticipate the consequences of the inevitable climate change to come.

References

Brasier, C. M., Robredo, F., & Ferraz, J. F. P. (1993). Evidence for Phytophthora cinnamomi involvement in Iberian oak decline. *Plant Pathology*, 42(1), 140-145.

Bronaugh, D. & Werner, A. (2013). zyp: Zhang + Yue-Pilon trends package. Pacific Climate Impacts Consortium. R package version 0.10-1. https://CRAN.R-project.org/package=zyp.

Caritat, A., Gutiérrez, E., & Molinas, M. (2000). Influence of weather on cork-ring width. *Tree physiology*, 20(13), 893-900.

Cerasoli, S., e Silva, F. C., & Silva, J. M. (2016). Temporal dynamics of spectral bioindicators evidence biological and ecological differences among functional types in a cork oak open woodland. *International journal of biometeorology*, 60(6), 813-825.

Correia, O. A., Oliveira, G. M., Martins-Loução, M. A., Catarino, F. M. (1992). Effects of bark-stripping on the water relations of Quercus suber L. *Scientia gerundensis*, 18: 195-204.

Costa, A., Pereira, H., & Oliveira, A. (2003). Variability of radial growth in cork oak adult trees under cork production. *Forest ecology and management*, 175(1-3), 239-246.

Costa, A., Pereira, H., & Madeira, M. (2009). Landscape dynamics in endangered cork oak woodlands in Southwestern Portugal (1958–2005). *Agroforestry Systems*, *77*(2), 83.

Costa, A., Pereira, H., & Madeira, M. (2010). Analysis of spatial patterns of oak decline in cork oak woodlands in Mediterranean conditions. *Annals of Forest Science*, 67(2), 204.

Costa-e-Silva, F., Correia, A. C., Piayda, A., Dubbert, M., Rebmann, C., Cuntz, M., Werner, C., David, J. S. & Pereira, J. S. (2015). Effects of an extremely dry winter on net ecosystem carbon exchange and tree phenology at a cork oak woodland. *Agricultural and forest meteorology*, 204, 48-57.

Da Silva, P. M., Aguiar, C. A., Niemelä, J., Sousa, J. P., & Serrano, A. R. (2009). Cork-oak woodlands as key-habitats for biodiversity conservation in Mediterranean landscapes: a case study using rove and ground beetles (Coleoptera: Staphylinidae, Carabidae). *Biodiversity and conservation*, 18(3), 605-619.

David, T. S., Henriques, M. O., Kurz-Besson, C., Nunes, J., Valente, F., Vaz, M., Pereira, J. S., Siegwolf, R., Chaves, M. M., Gazarini, L. C. & David, J. S. (2007). Water-use strategies in two co-occurring Mediterranean evergreen oaks: surviving the summer drought. *Tree physiology*, 27(6), 793-803.

Faias, S. P., Paulo, J. A., Palma, J. H., & Tomé, M. (2018). Understory effect on tree and cork growth in cork oak woodlands. *Forest systems*.

Ferreira, J. P. L. (2007). Models to predict the impact of the climate changes on aquifer recharge. *IAHS Publ*, 310, 103.

Godinho, S., Guiomar, N., Machado, R., Santos, P., Sá-Sousa, P., Fernandes, J. P., Neves N. & Pinto-Correia, T. (2016). Assessment of environment, land management, and spatial variables on recent changes in montado land cover in southern Portugal. *Agroforestry systems,* 90(1), 177-192.

Gouveia, A. C., & Freitas, H. (2008). Intraspecific competition and water use efficiency in Quercus suber: evidence of an optimum tree density?. *Trees*, 22(4), 521.

Häusler, M., Silva, J. M., Cerasoli, S., López-Saldaña, G., & Pereira, J. M. (2016). Modelling spectral reflectance of open cork oak woodland: a simulation analysis of the effects of vegetation structure and background. *International Journal of Remote Sensing*, *37*(3), 492-515.

ICNF (2013). IFN6 – Áreas dos usos do solo e das espécies florestais de Portugal continental. Resultados preliminares. *Instituto da Conservação da Natureza e das Florestas, Lisboa*, 34.

IUSS working group WRB. (2006). World reference base for soil resources 2006. *World soil resources reports* no. 103, 132-pp.

Joffre, R., & Rambal, S. (1993). How tree cover influences the water balance of Mediterranean rangelands. *Ecology*, 74(2), 570-582.

Ju, J., & Masek, J. G. (2016). The vegetation greenness trend in Canada and US Alaska from 1984–2012 Landsat data. *Remote Sensing of Environment*, 176, 1-16.

Ke, Y., Im, J., Lee, J., Gong, H., & Ryu, Y. (2015). Characteristics of Landsat 8 OLI-derived NDVI by comparison with multiple satellite sensors and in-situ observations. *Remote Sensing of Environment*, 164, 298-313.

Kendall, M. G. (1975). *Rank Correlation Methods*, Griffin, London.

Kim, H. N., Jin, H. Y., Kwak, M. J., Khaine, I., You, H. N., Lee, T. Y., Ahn, T. H., & Woo, S. Y. (2017). Why does Quercus suber species decline in Mediterranean areas?. *Journal of Asia-Pacific Biodiversity*, 10(3), 337-341.

Mann, H. B. (1945). Nonparametric tests against trend. *Econometrica: Journal of the Econometric Society*, 245-259.

Mendes, M. P., Ribeiro, L., David, T. S., & Costa, A. (2016). How dependent are cork oak (Quercus suber L.) woodlands on groundwater? A case study in southwestern Portugal. *Forest Ecology and Management*, 378, 122-130.

Moreno, G., Aviron, S., Berg, S., Crous-Duran, J., Franca, A., de Jalón, S. G., Hartel, T., Mirck, J., Pantera, A., Palma J. H. N., Paulo, J. A., Sanna, G. A. Re . F., Thenail, C., Varga, A., Viaud, V. & Burgess, P., J. (2017). Agroforestry systems of high nature and cultural value in Europe: provision of commercial goods and other ecosystem services. *Agroforestry Systems*, 1-15.

Natividade, J.V. (1950). Subericultura. Direcção Geral dos Serviços Florestais e Aquicolas, Lisbon.

Ogaya, R., Barbeta, A., Başnou, C., & Peñuelas, J. (2015). Satellite data as indicators of tree biomass growth and forest dieback in a Mediterranean holm oak forest. *Annals of forest science*, *72*(1), 135-144.

Paulo, J. A., & Tomé, M. (2010). Predicting mature cork biomass with t years of growth from one measurement taken at any other age. *Forest ecology and management*, 259(10), 1993-2005.

Paulo, J. A., Faias, S., Ventura-Giroux, C., & Tomé, M. (2015a). Estimation of stand crown cover using a generalized crown diameter model: application for the analysis of Portuguese cork oak stands stocking evolution. IForest. *Biogeosciences and Forestry*.

Paulo, J. A., Palma, J. H., Gomes, A. A., Faias, S. P., Tomé, J., & Tomé, M. (2015b). Predicting site index from climate and soil variables for cork oak (*Quercus suber L.*) stands in Portugal. *New forests*, 46(2), 293-307.

Paulo, J. A., Pereira, H., & Tomé, M. (2017). Analysis of variables influencing tree cork caliper in two consecutive cork extractions using cork growth index modelling. *Agroforestry systems*, 91(2), 221-237.

Pereira, H. (2007). Cork: biology, production and uses. *Elsevier*, Lisbon, 336.

Pettitt, A. N. (1979). A non-parametric approach to the change-point problem. *Applied statistics*, 126-135.

R Core Team (2017). R: A language and environment for statistical computing. R Foundation for Statistical Computing, Vienna, Austria. URL https://www.R-project.org/.

Rigueiro-Rodríguez, A., McAdam, J., & Mosquera-Losada, M. R. (Eds.). (2008). Agroforestry in Europe: current status and future prospects (Vol. 6). *Springer Science & Business Media*.

Romero, M. A., Sánchez, J. E., Jiménez, J. J., Belbahri, L., Trapero, A., Lefort, F., & Sánchez, M. E. (2007). New Pythium taxa causing root rot on Mediterranean Quercus species in South-west Spain and Portugal. *Journal of Phytopathology*, 155(5), 289-295.

Rouse Jr, J., Haas, R. H., Schell, J. A., & Deering, D. W. (1974). Monitoring vegetation systems in the Great Plains with ERTS.

Roy, D. P., Kovalskyy, V., Zhang, H. K., Vermote, E. F., Yan, L., Kumar, S. S., & Egorov, A. (2016). Characterization of Landsat-7 to Landsat-8 reflective wavelength and normalized difference vegetation index continuity. *Remote Sensing of Environment*, 185, 57-70.

Sen, P. K. (1968). Estimates of the regression coefficient based on Kendall's tau. *Journal of the American Statistical Association,* 63, 1379–1389.

She, X., Zhang, L., Cen, Y., Wu, T., Huang, C., & Baig, M. H. A. (2015). Comparison of the continuity of vegetation indices derived from Landsat 8 OLI and Landsat 7 ETM+ data among different vegetation types. *Remote Sensing*, 7(10), 13485-13506.

Silva, J. S. (2007). Os montados. Fundação Luso-Americana, *Público*, Lisboa.

Steven, M. D., Malthus, T. J., Baret, F., Xu, H., & Chopping, M. J. (2003). Intercalibration of vegetation indices from different sensor systems. *Remote Sensing of Environment*, 88(4), 412-422.

Teillet, P. M., Barker, J. L., Markham, B. L., Irish, R. R., Fedosejevs, G., & Storey, J. C. (2001). Radiometric cross-calibration of the Landsat-7 ETM+ and Landsat-5 TM sensors based on tandem data sets. *Remote sensing of Environment*, 78(1-2), 39-54.

Theil, H. (1950). A rank-invariant method of linear and polynomial regression analysis. *Nederlandse Akademie Wetenchappen Series,* A. 53, 386–392.

Pohlert, T. (2018). trend: Non-Parametric Trend Tests and Change-Point Detection. R package version 1.1.0. https://CRAN.R-project.org/package=trend.

Vaz, M., Pereira, J. S., Gazarini, L. C., David, T. S., David, J. S., Rodrigues, A. & Chaves, M. M. (2010). Drought-induced photosynthetic inhibition and autumn recovery in two Mediterranean oak species (Quercus ilex and Quercus suber). *Tree Physiology*, 30(8), 946-956.

Wang, J., Rich, P. M., Price, K. P., & Kettle, W. D. (2004). Relations between NDVI and tree productivity in the central Great Plains. *International Journal of Remote Sensing*, 25(16), 3127-3138.

Werner C, Correia O (1996) Photoinhibition in cork-oak leaves under stress: influence of the bark-stripping on the chlorophyll fluorescence emission in Quercus suber L. *Trees* 10: 288–292.

Zhu, Z., & Woodcock, C. E. (2012). Object-based cloud and cloud shadow detection in Landsat imagery. *Remote sensing of environment*, *118*, 83-94.

Appendix

Appendix 1: *Fmask* function coded in Google Earth Engine following pixel quality values.

Table of Landsat-5, -7 and -8 Surface Reflectance Pixel Quality Assessment (pixel_qa) band attributes, according to the USGS website. Full information can be found on https://landsat.usgs.gov/landsat-surface-reflectance-quality-assessment.

Bit	Bit Value	Cumulative Sum	Attribute
0	1	1	Fill
1	2	3	Clear
2	4	7	Water
3	8	15	Cloud Shadow
4	16	31	Snow
5	32	63	Cloud
6	64	127	Cloud Confidence 00 = none 01 = low 10 = medium 11 = high
7	128	255	

Function implemented in GEE to mask clouds and shadows, using the values of the table above.

```
var noclouds = function(image){

  // bit value for shadows is 8, bit value for clouds is 32
  var cloudShadowBitMask = ee.Number(2).pow(3).int();
  var cloudsBitMask = ee.Number(2).pow(5).int();

  // select the band 'pixel_qa' of the Landsat image
  var qa = image.select('pixel_qa');

  //select pixels with pixel_qa = 8 and 32 and give them a value of 0
  var mask = qa.bitwiseAnd(cloudShadowBitMask).eq(0)
      .and(qa.bitwiseAnd(cloudsBitMask).eq(0));

  // return the masked image
  var masked = image.updateMask(mask);
  return masked;
};
```

Appendix 2: Comparison of bands of Landsat and MODIS sensors.

Graphic of the band average relative spectral response of Landsat-7 (solid line), Landsat-8 (dash line) and MODIS (black). From the work on NDVI Landsat-8 characteristics by Ke *et al.*, 2015.

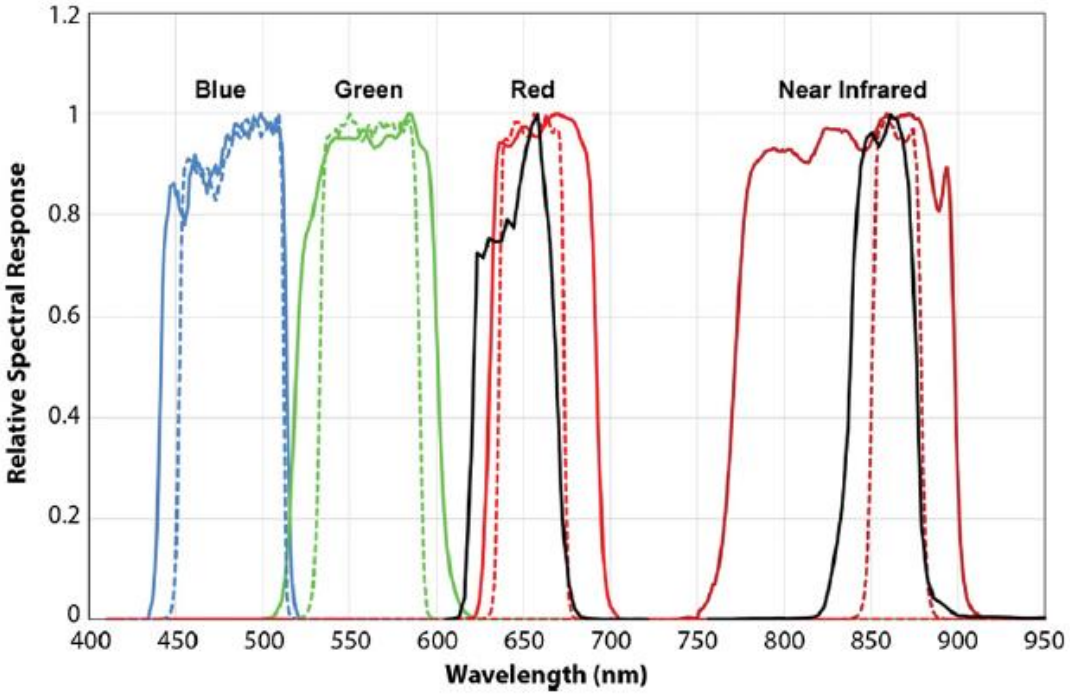

Table of comparison of bands thickness and resolution for four sensors. Can be noticed the huge difference of sensible wavelength between Near-infrared bands of Landsat-7 and -8. Regarding the sensibilities of the individual channels, it is expected closer NDVI values between Landsat-5, -7 and between Landsat-8 and MODIS.

Satellite	Band	Description	Wavelength	Resolution
Landsat-5	Band 1	Visible blue	0.45 to 0.52 µm	30-meter
	Band 3	Visible red	0.63 to 0.69 µm	30-meter
	Band 4	Near-infrared	0.76 to 0.90 µm	30-meter
Landsat-7	Band 1	Visible blue	0.45 to 0.52 µm	30-meter
	Band 3	Visible red	0.63 to 0.69 µm	30-meter
	Band 4	Near-infrared	0.77 to 0.90 µm	30-meter
Landsat-8	Band 2	Visible blue	0.450 to 0.515 µm	30-meter
	Band 4	Visible red	0.630 to 0.680 µm	30-meter
	Band 5	Near-infrared	0.845 to 0.885 µm	30-meter
MODIS	Band 3	Visible blue	0.459 to 0.479 µm	500-meter
	Band 1	Visible red	0.620 to 0.670 µm	250-meter
	Band 2	Near-infrared	0.841 to 0.876 µm	250-meter

Appendix 3: Comparison of NDVI values for cork oaks, herbaceous and shrubs along years.

3.a. Annual evolution of the values of NDVIs for herbaceous and cork oaks (Cerasoli *et al*., 2016).

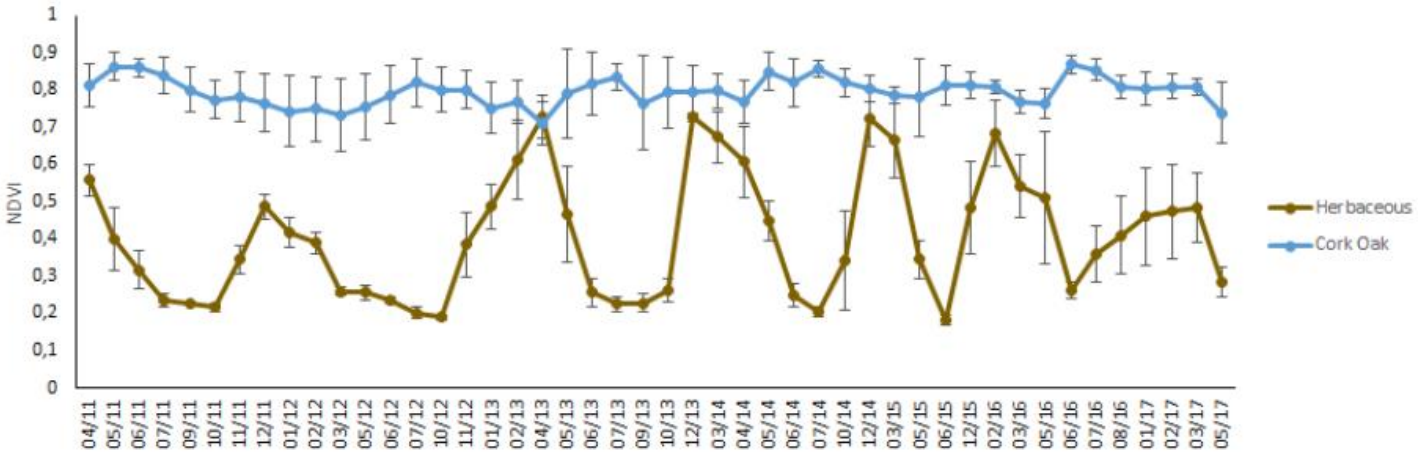

3.b. Annual evolution of the values of NDVIs for *Cistus salviifolius* and *Ulex airensis* (Cerasoli *et al*., 2016).

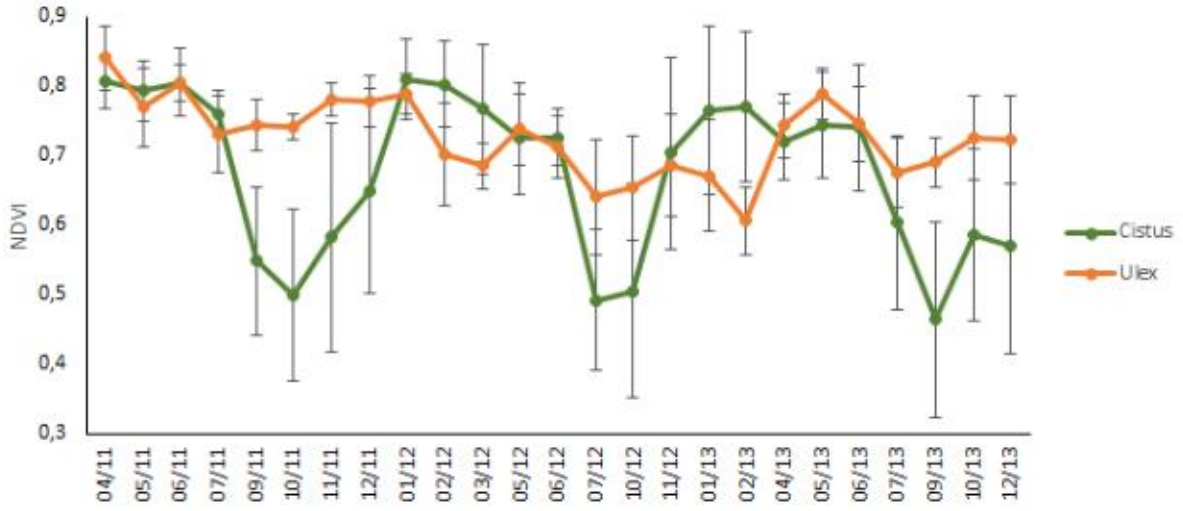

Appendix 4: Normal Q-Q plots for the six study-site, for Landsat-5, -7 and -8 derived-NDVI raw-values.

The red line represents the expected result for a population following a Normal distribution.

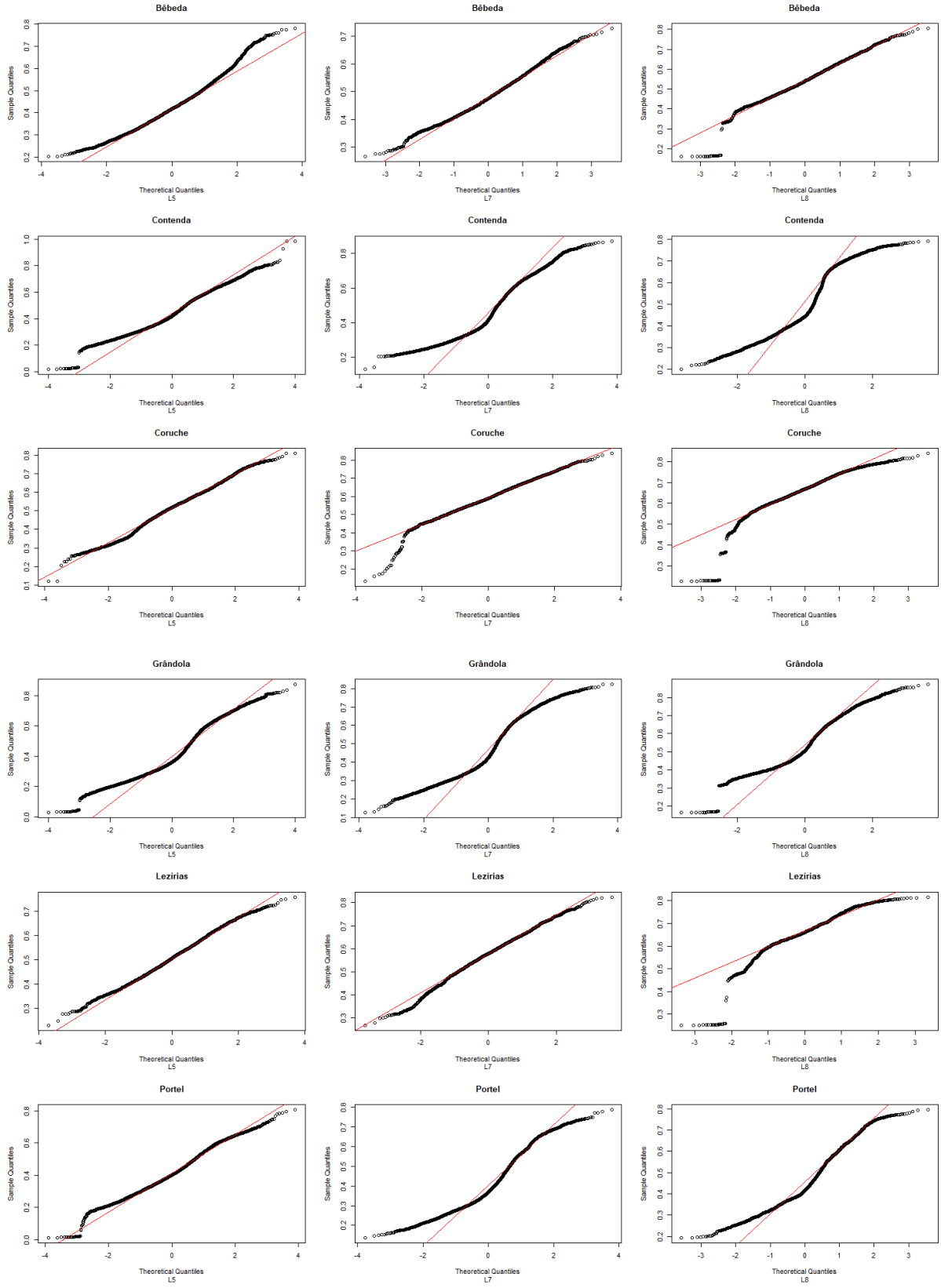

Appendix 5: Boxplots to compare the accuracy of NDVI adjustment equations between Landsat-5, -7 and -8 sensors.

On the left, boxplots of Landsat-5 (L5, red) and Landsat-7 (L7, violet) for each equation. On the right, boxplots of Landsat-8 (L8, light-blue) and Landsat-7 (L7, violet). Are represented per each box the quartiles and the median, in a grey cross the mean. The values of means (grey) and medians (blacks) are written under each box.

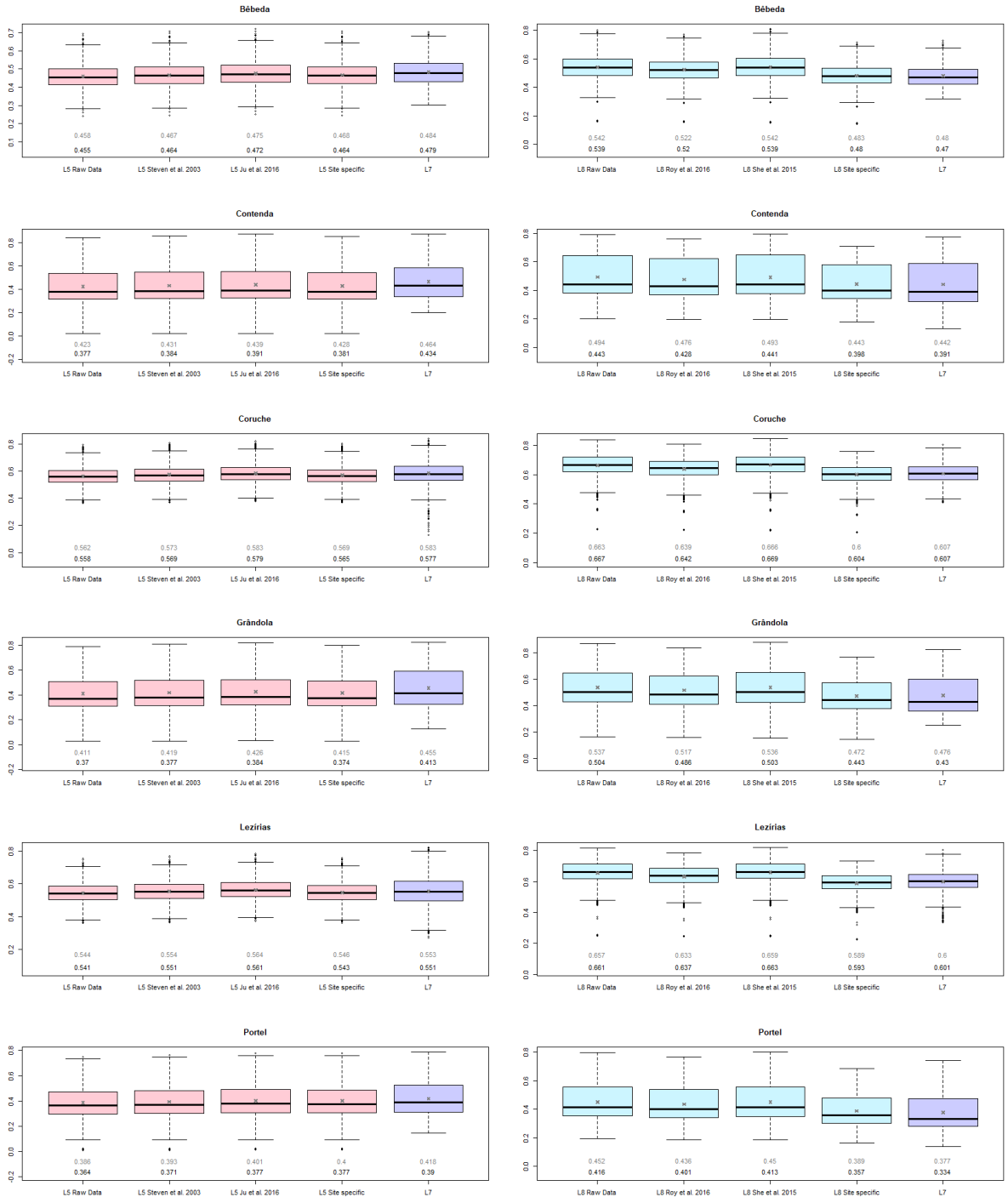

Appendix 6: Comparison of adjusted and not-adjusted Landsat -5 and -8 NDVIs.

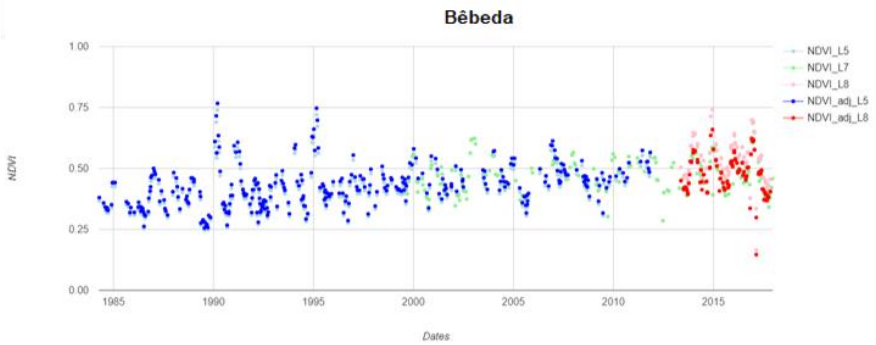

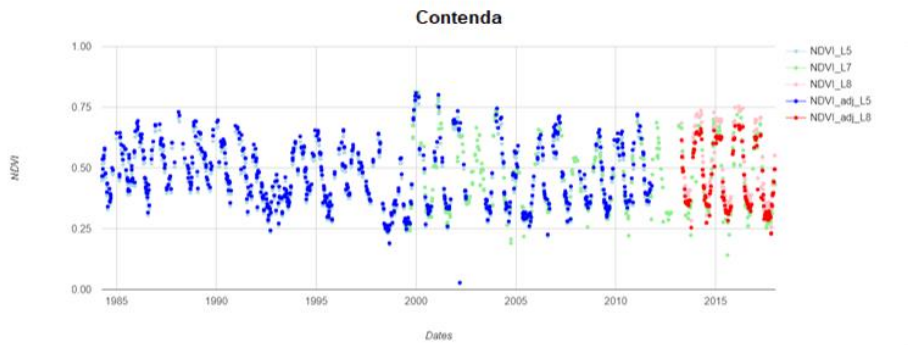

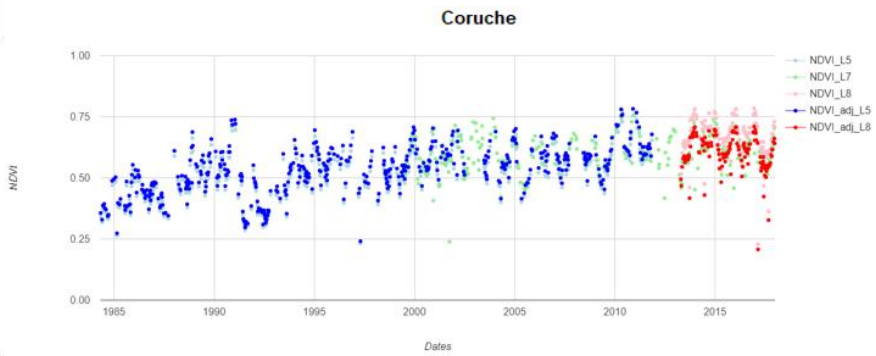

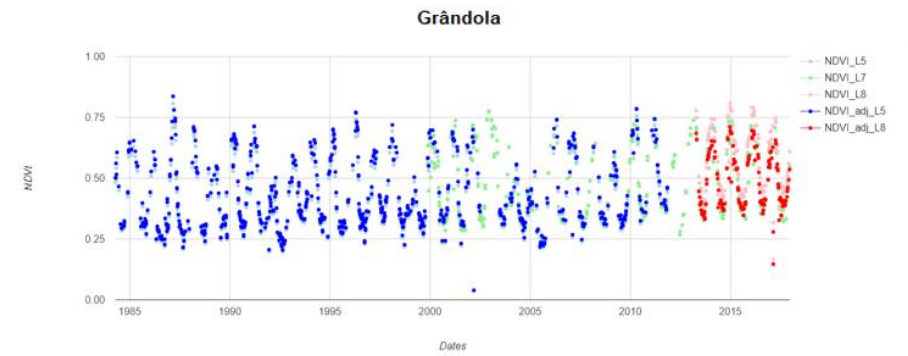

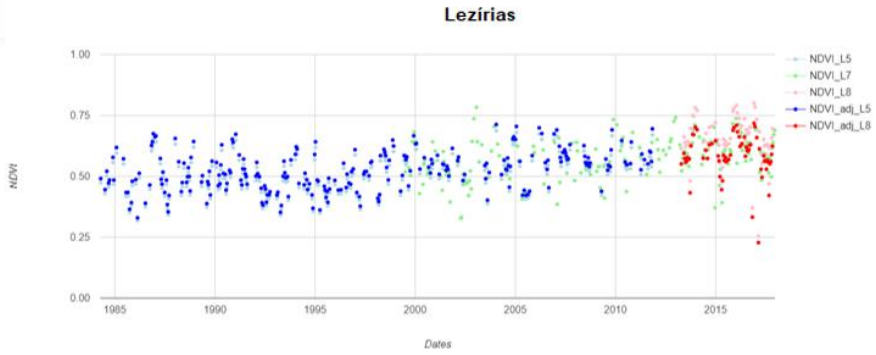

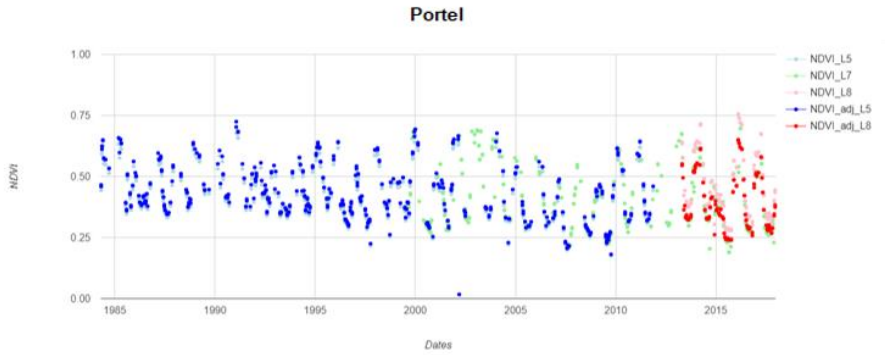

Appendix 7: Matches between the classes kept (Code) and the original classes of the Portuguese land use and land cover maps (*Carta de Uso e Ocupação do Solo* (COS)) for 1995, 2007-2010 and 2015 classifications.

Code	COS 1995	COS 2007 – COS 2010	COS 2015
1	3.1.1.01.1 Florestas de sobreiro	2.4.4.04.1 SAF de sobreiro com culturas permanentes	3.1.1.00.1 Florestas de sobreiro
1	3.1.1.01.1 Florestas de sobreiro	3.1.1.01.1 Florestas de sobreiro	3.1.1.00.1 Florestas de sobreiro
1	3.1.1.01.1 Florestas de sobreiro	3.1.1.02.1 Florestas de sobreiro com folhosas	3.1.1.00.1 Florestas de sobreiro
1	3.1.1.01.1 Florestas de sobreiro	3.1.3.01.1 Florestas de sobreiro com resinosas	3.1.1.00.1 Florestas de sobreiro
1	3.1.1.01.1 Florestas de sobreiro	3.2.4.01.1 Florestas abertas de sobreiro	3.1.1.00.1 Florestas de sobreiro
1	3.1.1.01.1 Florestas de sobreiro	3.2.4.02.1 Florestas abertas de sobreiro com folhosas	3.1.1.00.1 Florestas de sobreiro
1	3.1.1.01.1 Florestas de sobreiro	3.2.4.05.1 Florestas abertas de sobreiro com resinosas	3.1.1.00.1 Florestas de sobreiro
1	3.2.4.08.1 Cortes rasos de florestas de sobreiro	3.2.4.08.1 Cortes rasos de florestas de sobreiro	3.1.1.00.1 Florestas de sobreiro
1	3.2.4.10.1 Novas plantações de florestas de sobreiro	3.2.4.10.1 Novas plantações de florestas de sobreiro	3.1.1.00.1 Florestas de sobreiro
1	3.3.4.02.1 Áreas ardidas de florestas de sobreiro	3.3.4.02.1 Áreas ardidas em florestas de sobreiro	3.1.1.00.1 Florestas de sobreiro
2	3.1.1.01.2 Florestas de azinheira	2.4.4.04.2 SAF de azinheira com culturas permanentes	3.1.1.00.2 Florestas de azinheira
2	3.1.1.01.2 Florestas de azinheira	3.1.1.01.2 Florestas de azinheira	3.1.1.00.2 Florestas de azinheira
2	3.1.1.01.2 Florestas de azinheira	3.1.1.02.2 Florestas de azinheira com folhosas	3.1.1.00.2 Florestas de azinheira
2	3.1.1.01.2 Florestas de azinheira	3.1.3.01.2 Florestas de azinheira com resinosas	3.1.1.00.2 Florestas de azinheira
2	3.1.1.01.2 Florestas de azinheira	3.2.4.01.2 Florestas abertas de azinheira	3.1.1.00.2 Florestas de azinheira
2	3.1.1.01.2 Florestas de azinheira	3.2.4.02.2 Florestas abertas de azinheira com folhosas	3.1.1.00.2 Florestas de azinheira
2	3.1.1.01.2 Florestas de azinheira	3.2.4.05.2 Florestas abertas de azinheira com resinosas	3.1.1.00.2 Florestas de azinheira
2	3.2.4.08.2 Cortes rasos de florestas de azinheira	3.2.4.08.2 Cortes rasos de florestas de azinheira	3.1.1.00.2 Florestas de azinheira
2	3.2.4.10.2 Novas plantações de florestas de azinheira	3.2.4.10.2 Novas plantações de florestas de azinheira	3.1.1.00.2 Florestas de azinheira
2	3.3.4.02.2 Áreas ardidas de florestasde azinheira	3.3.4.02.2 Áreas ardidas em florestasde azinheira	3.1.1.00.2 Florestas de azinheira
3	2.4.4.01.1 SAF de sobreiro com culturas temporárias de sequeiro	2.4.4.01.1 SAF de sobreiro com culturas temporárias de sequeiro	2.4.4.00.1 SAF de sobreiro
3	2.4.4.02.1 SAF de sobreiro com culturas temporárias de regadio	2.4.4.02.1 SAF de sobreiro com culturas temporárias de regadio	2.4.4.00.1 SAF de sobreiro
3	2.4.4.03.1 SAF de sobreiro com pastagens	2.4.4.03.1 SAF de sobreiro com pastagens	2.4.4.00.1 SAF de sobreiro
4	2.4.4.01.2 SAF de azinheira com culturas temporárias de sequeiro	2.4.4.01.2 SAF de azinheira com culturas temporárias de sequeiro	2.4.4.00.2 SAF de azinheira
4	2.4.4.02.2 SAF de azinheira com culturas temporárias de regadio	2.4.4.02.2 SAF de azinheira com culturas temporárias de regadio	2.4.4.00.2 SAF de azinheira
4	2.4.4.03.2 SAF de azinheira com pastagens	2.4.4.03.2 SAF de azinheira com pastagens	2.4.4.00.2 SAF de azinheira
5	2.4.4.01.6 SAF de sobreiro com azinheira e com culturas temporárias de sequeiro	2.4.4.01.6 SAF de sobreiro com azinheira e com culturas temporárias de sequeiro	2.4.4.00.6 SAF de sobreiro com azinheira
5	2.4.4.02.6 SAF de sobreiro com azinheira e com culturas temporárias de regadio	2.4.4.02.6 SAF de sobreiro com azinheira e com culturas temporárias de regadio	2.4.4.00.6 SAF de sobreiro com azinheira
5	2.4.4.03.6 SAF de sobreiro com azinheira com pastagens	2.4.4.03.6 SAF de sobreiro com azinheira com pastagens	2.4.4.00.6 SAF de sobreiro com azinheira
5	2.4.4.04.6 SAF de sobreiro com azinheira com culturas permanentes	2.4.4.04.6 SAF de sobreiro com azinheira com culturas permanentes	2.4.4.00.6 SAF de sobreiro com azinheira

Appendix 8: Evolution of area covered per each class of land cover, and comparison with the amount of constant areas of each class.

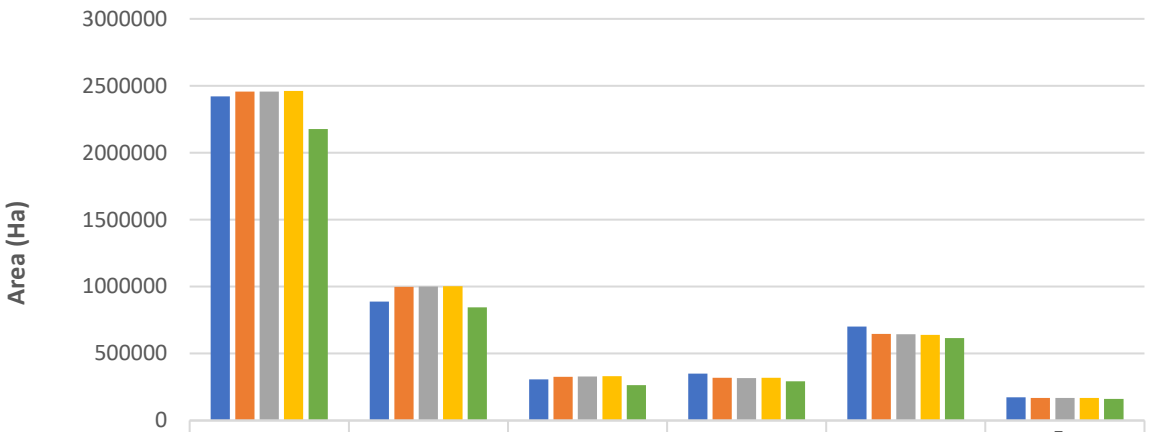

	All classes	1 - Cork oak forests	2 - Holm oak forests	3 - Cork oak agroforestry systems	4 - Holm oak agroforestry systems	5 - Agroforestry systems with both species
COS 1995	2419905.69	887046.03	308152.44	350156.97	701878.05	172672.2
COS 2007	2457255.87	997058.61	326661.66	318064.23	646995.69	168475.68
COS 2010	2456964.72	1000068.66	328146.75	316887.84	643572.72	168288.75
COS 2015	2461966.65	1003461.84	330888.6	318454.38	640522.44	168639.39
Constant areas	2177116.74	844152.93	264895.74	292333.59	614576.79	161157.69

COS: Land use and land cover map of Portugal (Carta de Uso e Ocupação do Solo).

The area covered by oaks increases from 1995 to 2015. More precisely, cork oak forests won 100,000 hectares and holm oak 20,000 ha between 1995 and 2007, due to public policies and change of production means. Meanwhile, cork oak and holm oak agroforestry system areas lost altogether 90,000 ha the first 12 years and keep decreasing afterward.

The constant areas (in green) are more than 80% of the maximum area covered by the land cover class along the COS, for every class.

Appendix 9: Enlargement of the masks of constant land cover classes and burned areas.

Images presented in **Figure 7** of the main document.

9.a. Cork oak and holm oak constant areas in Portugal (1995 - 2015), from Land Use and Land Cover Maps of Portugal of 1995, 2007, 2010 and 2015. Pixel size: 30m². Minimum map unit: 1 ha.

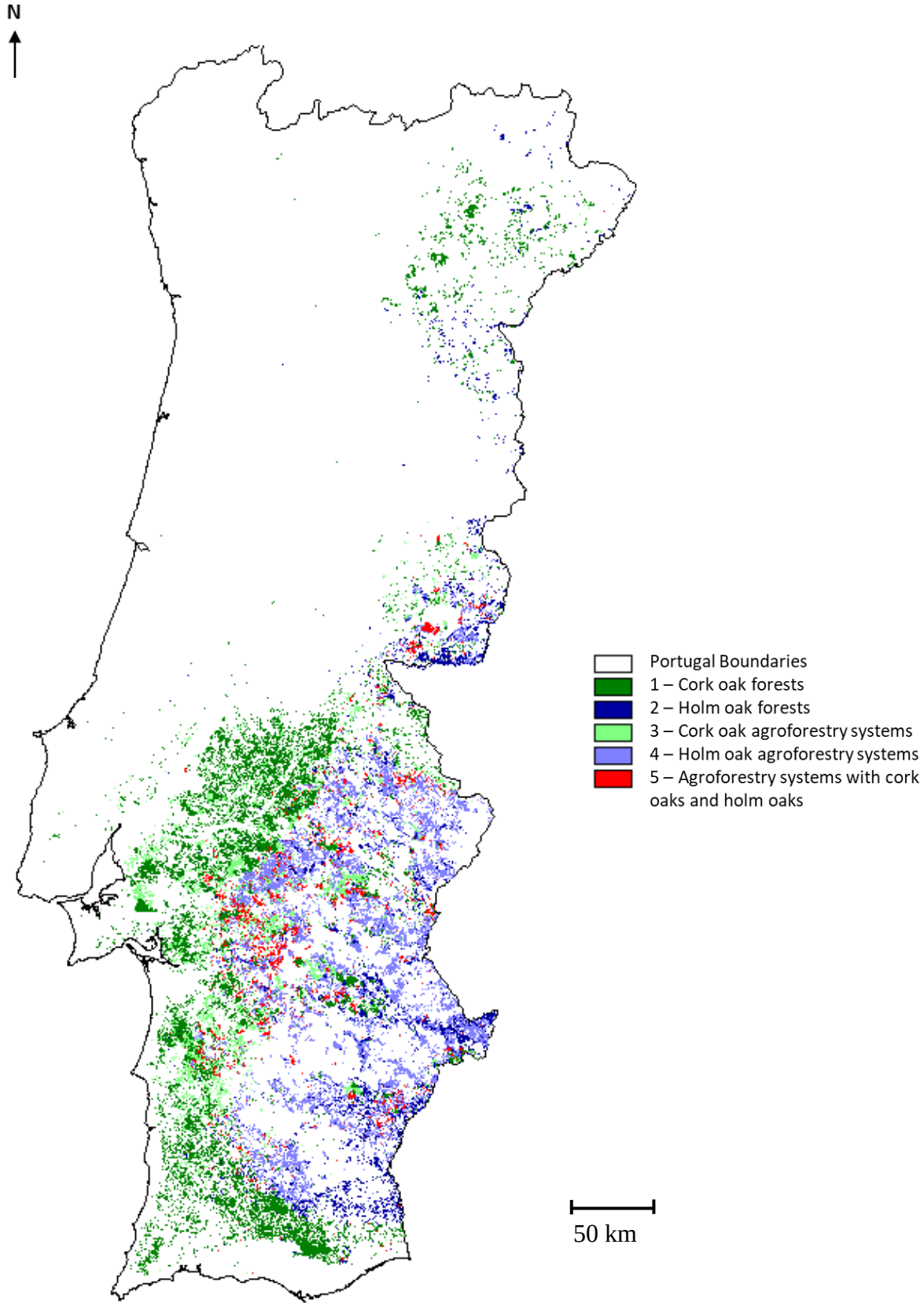

9.b. Burned areas in continental Portugal (1984 and 2017), from annual burned areas maps of the Nature and Forests Conservation Portuguese Institute (Instituto da Conservação da Natureza e das Florestas, ICNF). Pixel size: 30m². Minimum map unit: 5 ha.

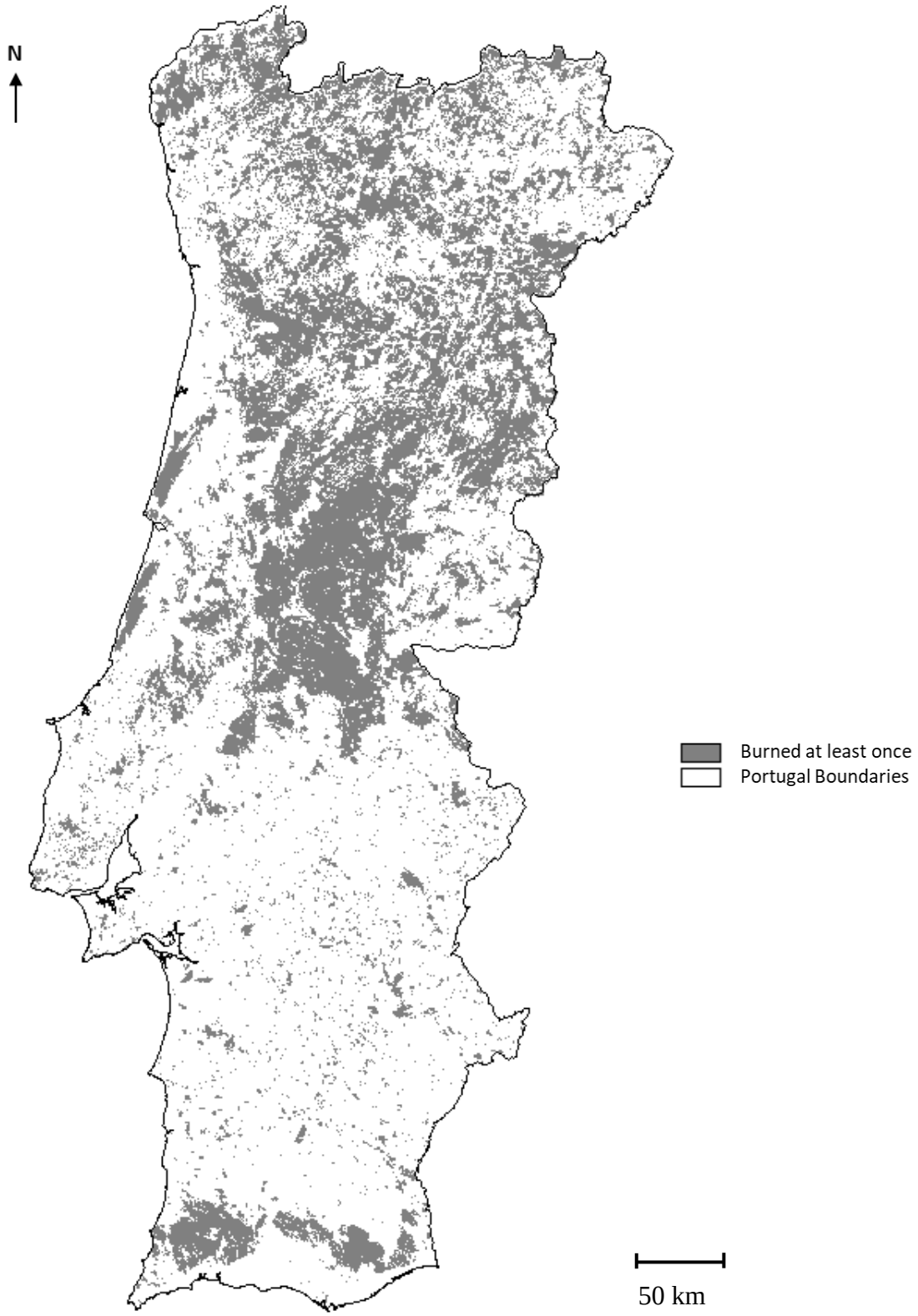

Appendix 10: Enlargement of Theil Sen slopes and Mann-Kendall significance maps per land cover class.

Images presented in **Figure 11** of the main document. Presented in class numerical order, as followed: 1: Cork oak forests, 2: Holm oak forests, 3: Cork oak Agroforestry systems, 4: Holm oak agroforestry systems, 5: Agroforestry systems with cork and holm oak. Pixel representative size: 30m².

10.a. Class 1 – Cork oak forests.

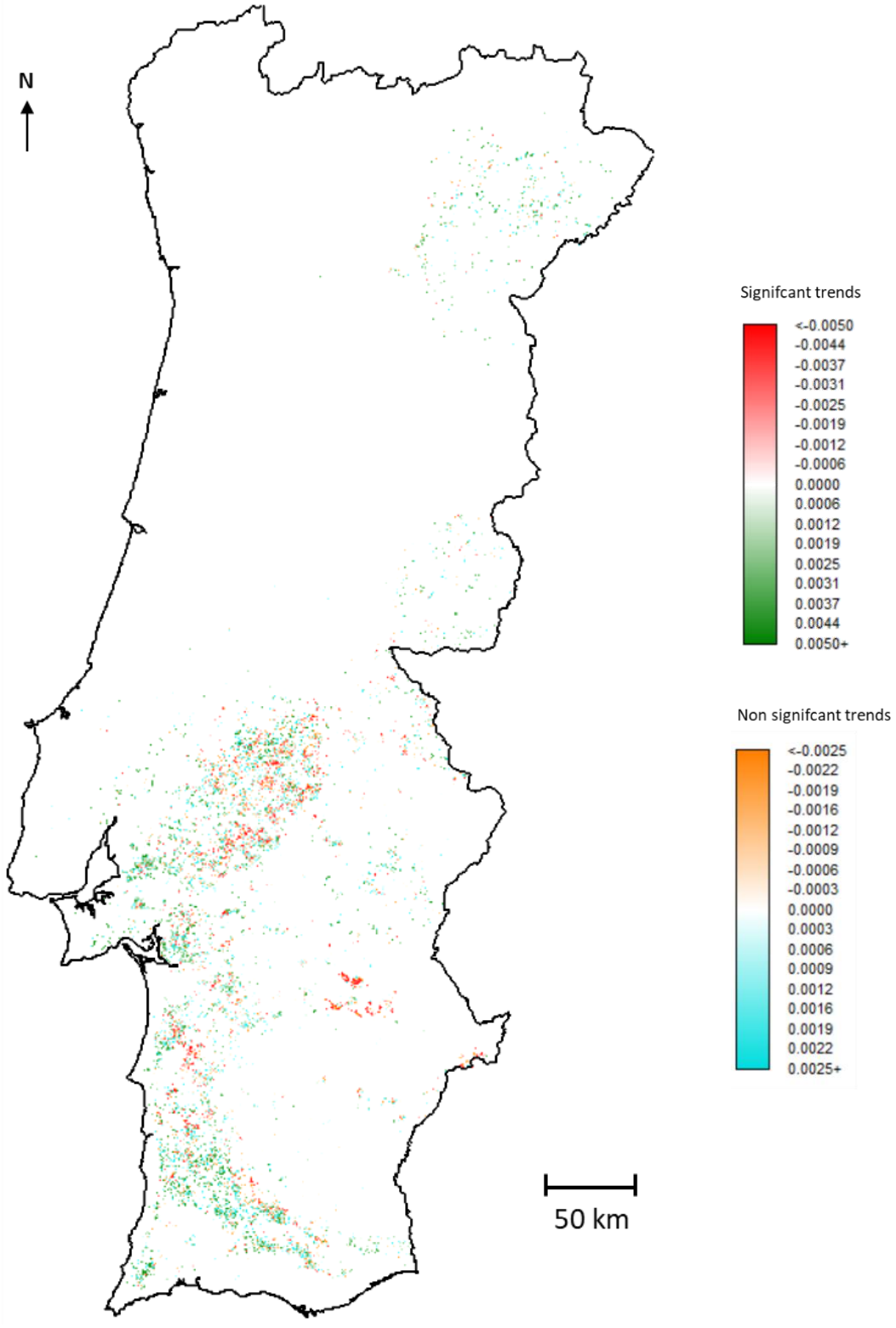

10.b. Class 2 – Holm oak forests.

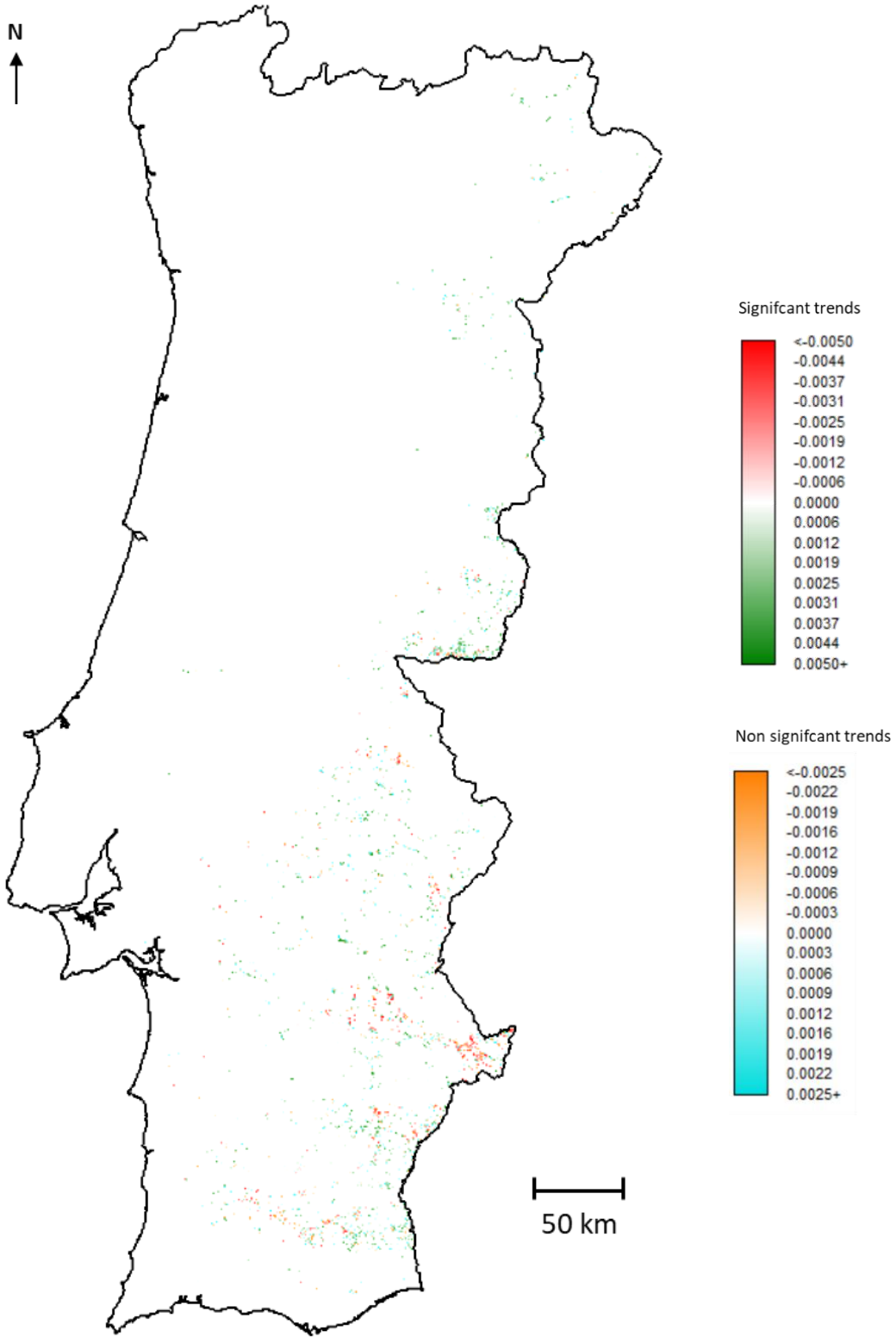

10.c. Class 3 – Cork oak agroforestry systems.

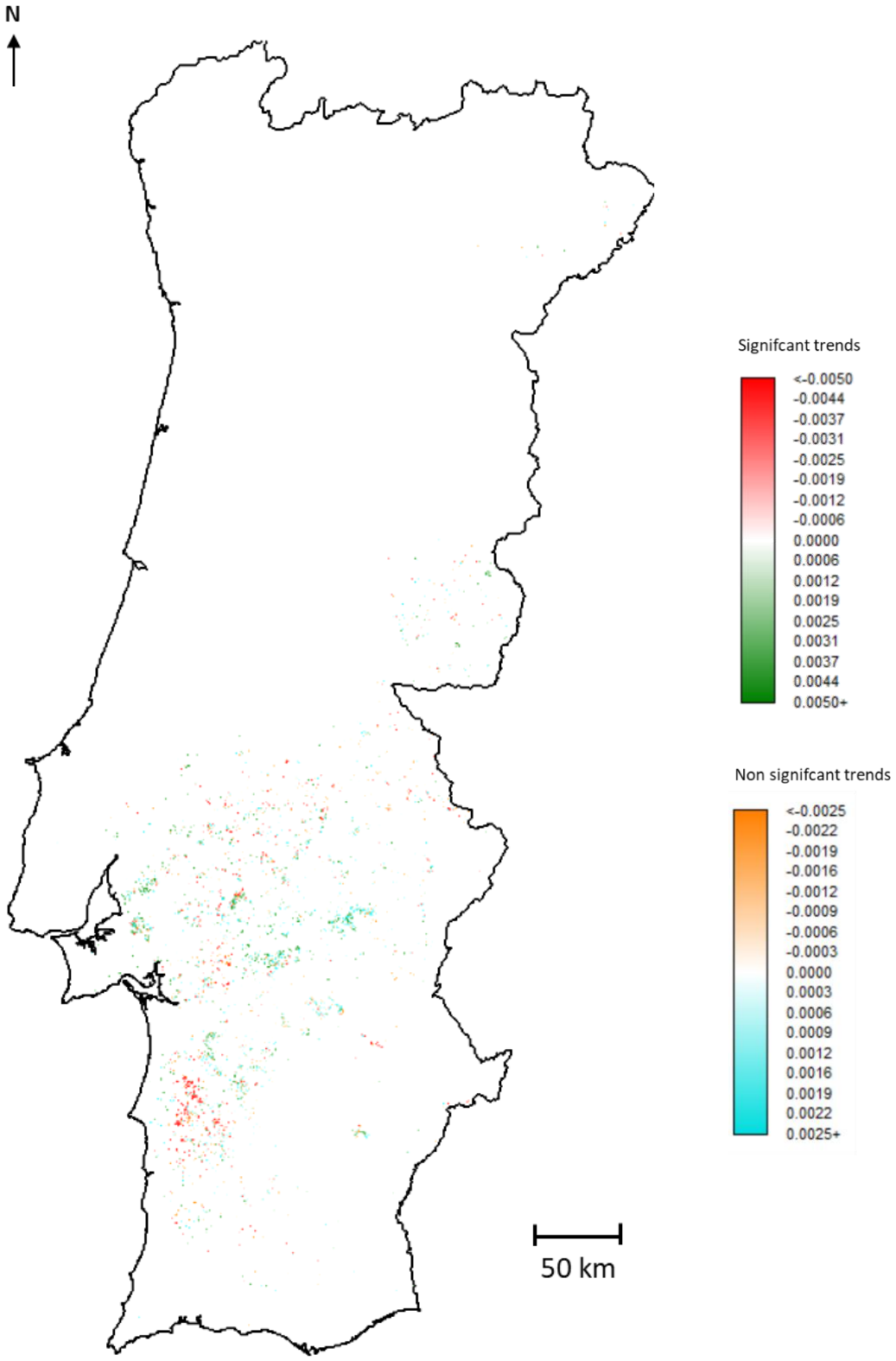

10.d. Class 4 – Holm oak agroforestry systems.

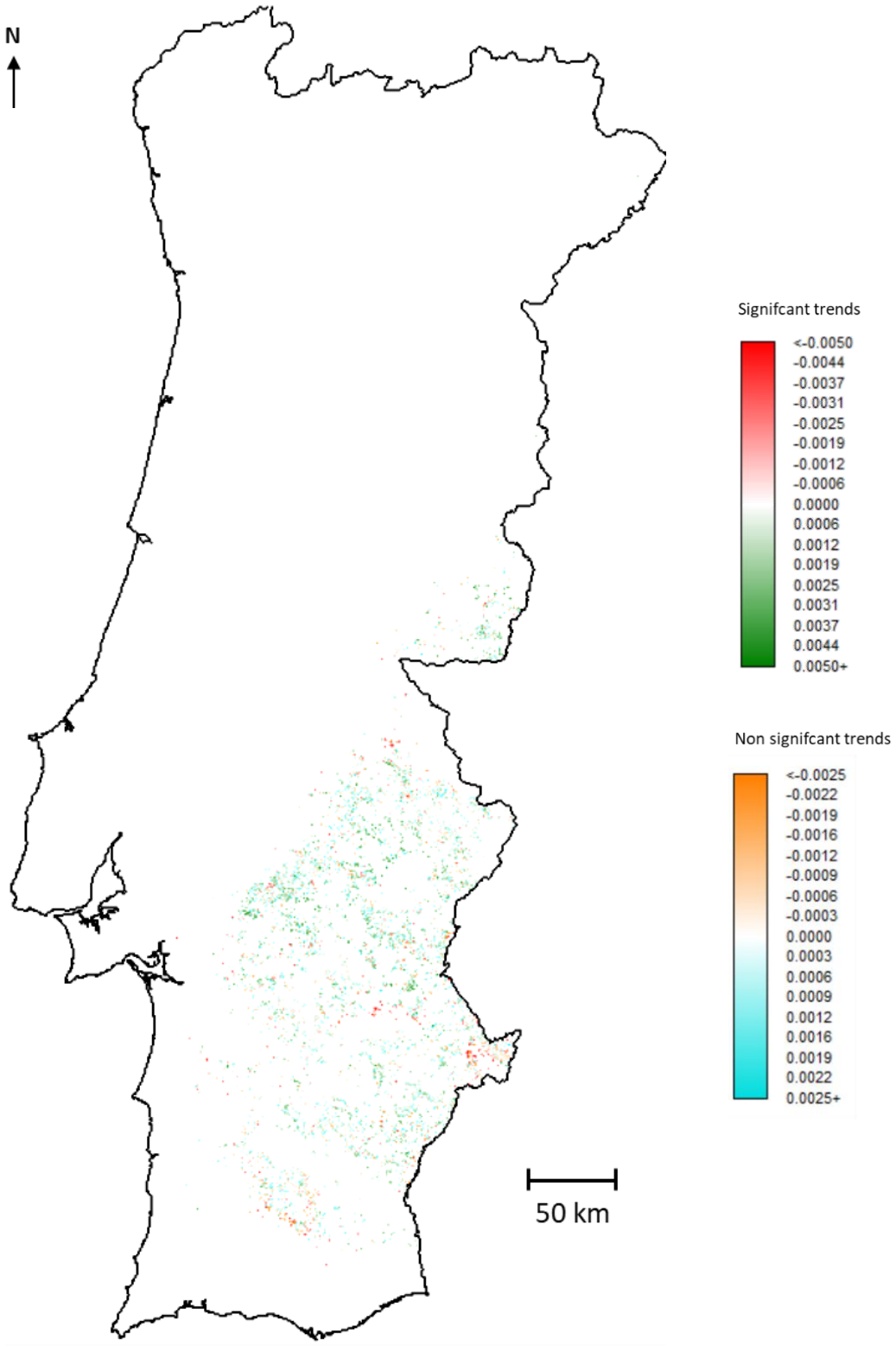

10.e. Class 5 – Cork and holm oak agroforestry systems.

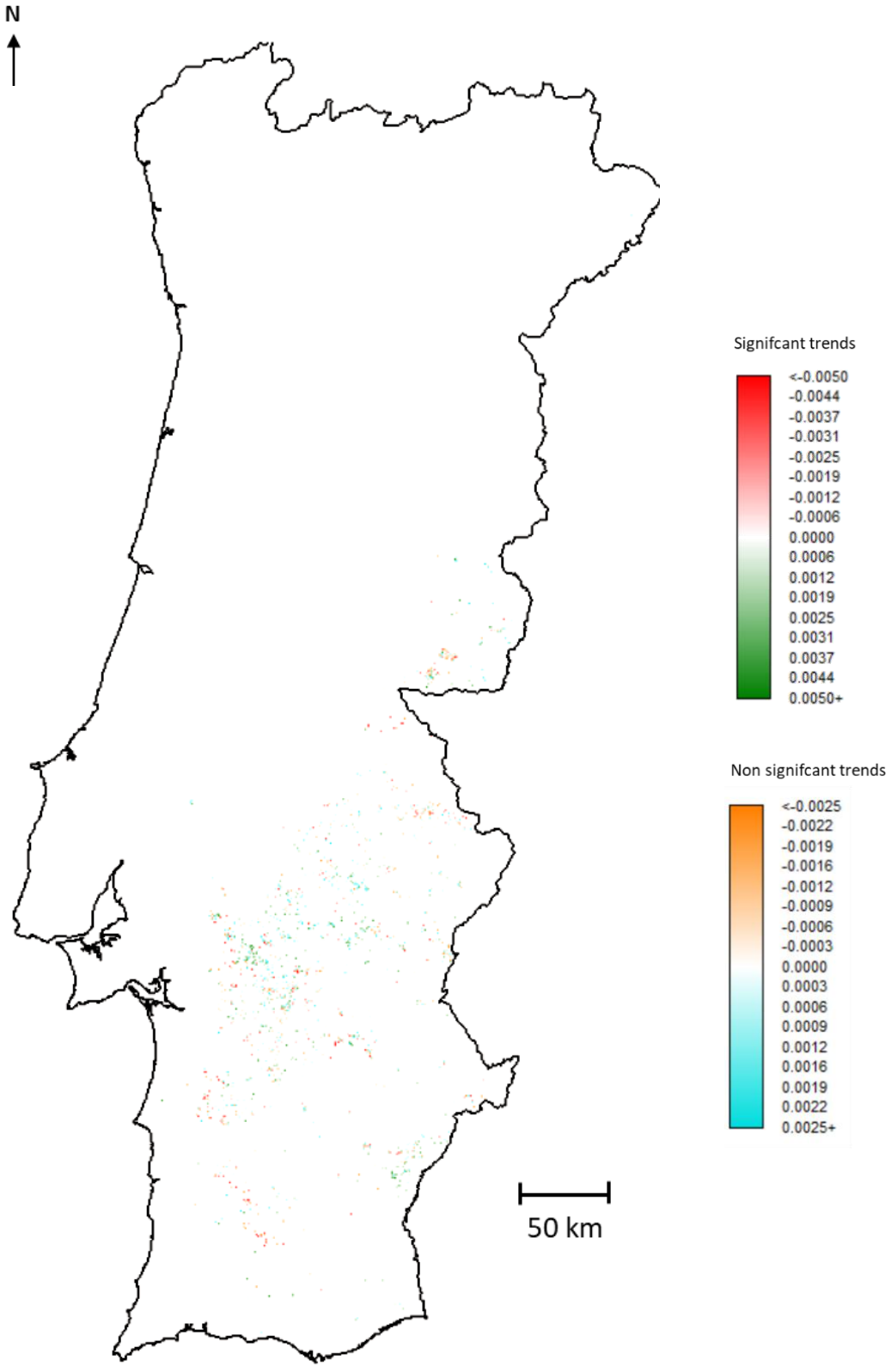

Appendix 11: Frequency histograms of all slopes and significant slopes values for each land cover class.

Class 1: Cork oak forests, 2: Holm oak forests, 3: Cork oak Agroforestry systems, 4: Holm oak agroforestry systems, 5: Agroforestry systems with cork and holm oak.

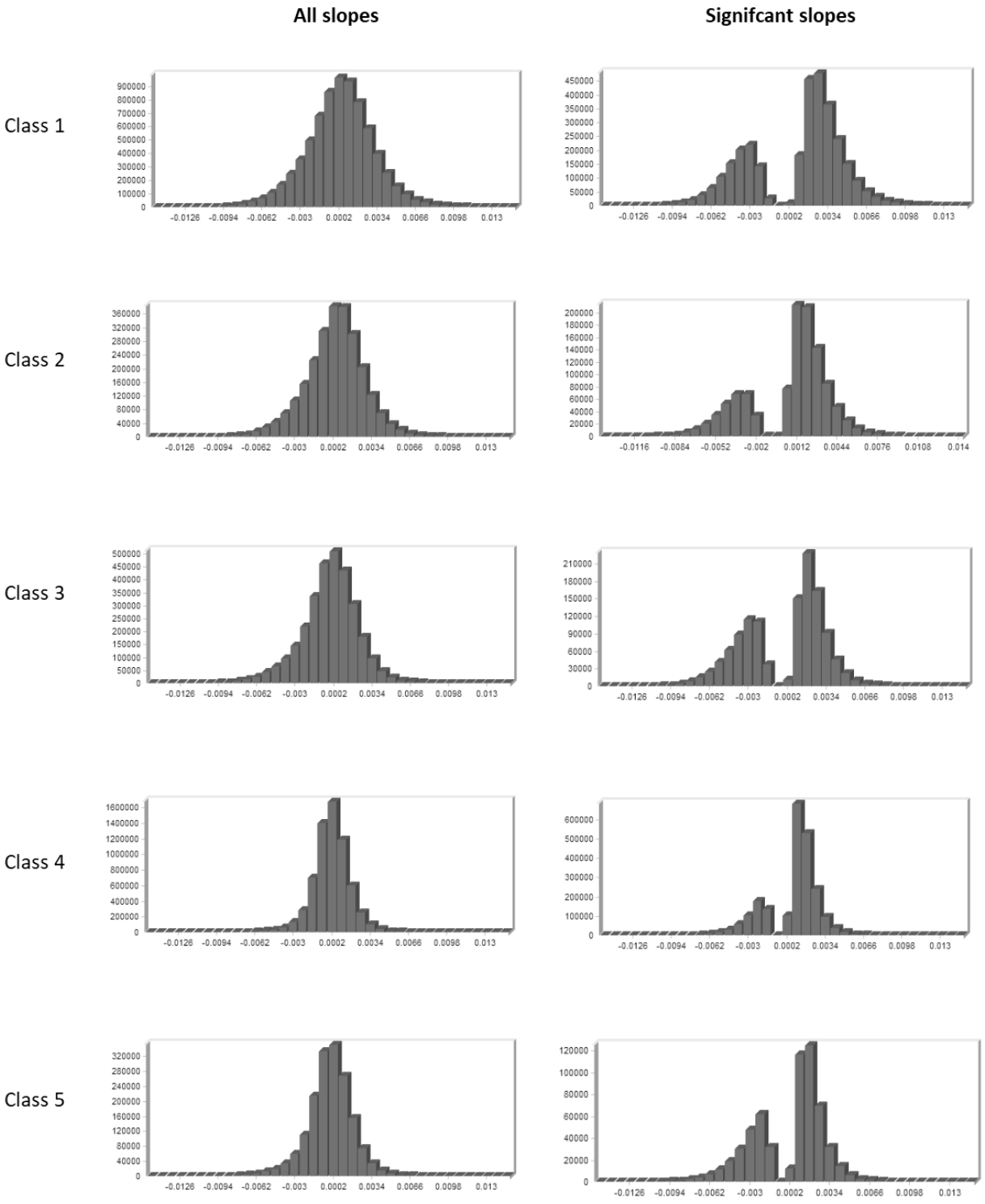

	Diplôme : Ingénieur agronome, agroalimentaire et territorial Spécialité : Agronomie Spécialisation / option : Télédétection et Environnement (TELENVI) Enseignant référent : Hervé Nicolas

Auteur : Valentine AUBARD Date de naissance : 13/09/1995	Organisme d'accueil : Insituto Superior de Agronomia (ISA) Adresse : Tapada da Ajuda, 1349-017 Lisboa Maîtres de stage : João Manual Das Neves Silva et Joana Amaral Paulo
Nb pages : 30 Annexe(s) :16	
Année de soutenance : 2018	

Titre français : Suivi des bois de chênes lièges et chênes verts avec Google Earth Engine

Titre anglais : Monitoring cork and holm oak woodlands with Google Earth Engine

Résumé (1600 caractères maximum) : Les bois de chênes du Sud de l'Europe sont considérés être en déclin. Afin de quantifier ce phénomène, les tendances sur 34 ans de l'indice de végétation par différence normalisé (NDVI) ont été cartographiées à une précision de 30 mètres, pour l'ensemble des forêts de chênes lièges (*Quercus suber*) et de chênes verts (*Q. ilex*) du Portugal continental. L'indice NDVI est un bon proxy pour suivre la santé et la productivité des arbres au cours du temps. Les images de Landsat 5, 7 et 8 ont été utilisées pour obtenir une série temporelle de 1984 à 2017. Les NDVI de MODIS servirent de comparaison après l'an 2000. Google Earth Engine permet d'utiliser librement ces images. Les valeurs de NDVI de Landsat 5 et 8 furent ajustées à celles de Landsat 7. Pour minimiser l'impact spectral de la végétation de sous étage, seuls les NDVI de Juillet et Août furent utilisés. Les tests de Mann-Kendall (MK) et contextuel de MK ont permis d'estimer la significativité et le signe des tendances, et l'estimateur de Theil-Sen (TS) les pentes. Cette méthodologie a d'abord été testée sur six parcelles de chênes lièges. Des modèles linéaires ont montré l'effet significatif des précipitations et de l'extraction du liège sur les variations de NDVI. Un test de Pettitt révéla des ruptures de tendance significatives autour de l'an 2000. Pour le pays entier, une analyse spatio-temporelle a été réalisée sur les parcelles stables de chênes lièges et verts. Trente pour cent présentent des tendances décroissantes, surtout dans le Centro et l'Alentejo littoral et intérieur.

Abstract (1600 caractères maximum) : Oak woodlands are being documented to be declining in southern Europe. In order to verify and quantify this phenomenon, 34-year trends of the Normalized Difference Vegetation Index (NDVI) were calculated and mapped at 30-meter pixel scale for all cork oak (Quercus suber) and holm oak (Quercus ilex) areas of continental Portugal. NDVI is considered a good proxy to monitor trees health and productivity along years. Landsat 5, 7 and 8 imagery from 1984 to 2017 were used to derive a long-term NDVI time series. MODIS 250-m spatial resolution NDVI product was used to compare values for the period after 2000. All imagery were freely available and treatable on Google Earth Engine. NDVI values of Landsat 5 and 8 were adjusted to Landsat 7 values. Only July and August NDVI were used to minimize the spectral contribution of understorey vegetation and its phenological variability, thus focusing on the tree layer. Signs and significance of trends were calculated by Mann-Kendall (MK) and contextual MK tests, and their slopes using Theil-Sen (TS) estimator. The methodological approach was first tested on six cork oaks stands. Linear models revealed the effect of annual cumulated precipitation and debarking on NDVI variations. All trends were found significant. A Pettitt test showed significant change-points around the year 2000. At country scale, a spatio-temporal trend analysis was performed on stable cover areas of holm and cork oak. Thirty percent of woodlands area presents declining trends, mainly located in Centro region, and interior and littoral of Alentejo.

Mots-clés : *Quercus suber L., Quercus ilex L.,* Montado, Série Temporelle, indice de végétation NDVI, Mann-Kendall contextuel, Portugal

Key Words: *Quercus suber L., Quercus ilex L.,* Montado, Time series, Normalized Difference Vegetation Index, Contextual Mann-Kendall, Portugal